University of Zurich[UZH]

Influence of temperature and VPD on d2H in leaves of plants with different carbon fixation pathways

ESS 511 Master's Thesis

Author
Oliver Rehmann
13-053-673

Supervised by
Marco Lehmann (marco.lehmann@wsl.ch)
Philipp Schuler (pschuler@student.ethz.ch)

Faculty representative
PD Dr. Guido Lars Bruno Wiesenberg

30.04.2022
Department of Geography, University of Zurich

University of Zurich[UZH]

Eidg. Forschungsanstalt für Wald, Schnee und Landschaft WSL

Influence of temperature and VPD on δ^2H in leaves of plants with different carbon fixation pathways

Master Thesis

Earth System Sciences, UZH Zurich

Zurich, April 30, 2022

Author: Oliver Rehmann (13-053-673)
oliver.rehmann@uzh.ch

Abstract

The investigation of moisture stress and photosynthetic activity in earths ecosystems has become more important in recent years due to the changing climate. Stable isotope represent a versatile tool to observe bio-physiological relationships. However, the processes that shape isotope signals have not been fully understood. Especially stable hydrogen isotopes analysis in non structural carbohydrates have not been studied extensively because of the lack of viable methods.

In this thesis, I try to give more insight on the fractionation processes of stable hydrogen isotopes in different plant compounds of varying carbon fixation pathways and their behaviour under distinct environmental conditions (temperature, VPD). I was able to show, that separate carbon fixation pathways exhibit significant differences in ^{2}H composition with an enrichment in warmer and drier conditions. Furthermore, the analysis of $\delta^2H_{(ne)}$ lead to the assumption that the ^{2}H cellulose composition is mostly dependent on the sugar composition but is also affected by temperature and VPD.

Additionally, the biological fractionation factors could be use to measure plant performance. But also to distinguish between different carbon fixation pathways and detect facultative CAM species. This knowledge could lead to a better predictions of how ecosystems react to climate change and thus how their carbon fixation ability might change in the future.

Contents

List of Figures

List of Tables

Chapter 1

Introduction

1.1 Motivation

In recent years, numerous papers have been published about the processes and implication of climate change. Last year, for the first time the turnover from a net carbon sink to a carbon source of the Amazonian rain forest was observed (Gatti et al., 2021). One of the reasons stated is moisture stress, that could lead to increased tree mortality and a reduction of photosynthetic rate. A versatile approach of investigating bio-physiological relationships and effects are stable isotopes (Dulamsuren & Hauck, 2021). Stable isotopes, such as from ^{18}O and ^{13}C have been used extensively as dendrochronological proxies and to understand physical processes such as water exchange and carbon fixation pathways (Saurer et al., 1997; Saurer & Cherubini, 2021; Tcherkez et al., 2011; Xia et al., 2020). This knowledge is vital for a better understanding of how ecosystems might react to changing precipitation patterns and increasing droughts in the future (Naumann et al., 2018). However, especially in hydrogen stable isotope research, many processes are not yet fully understood. In this context, the following thesis aims to identify how the δ^2H signal changes from the leaf water to the primary assimilates (e.g. sugars) and at last cellulose. Especially, the analysis of sugars has not be done extensively because of technical limitations (Schuler et al., 2021). However, to be able to understand the empirical part of the thesis, one needs to understand what isotopes are and how they might be used for research.

1.2 Isotopes

1.2.1 What are isotopes?

All elements are structured the same way, and consist of the same subatomic particles which are protons (positive charge), electrons (negative charge) and neutrons (no charge) (Sharp, 2007). Each element has a different number of protons. In a neutral atom, there are an equal amount of protons and electrons. The atomic mass, however, is mostly affected by the amount of protons and neutrons. The weight of electrons is negligible.

Now, isotopes are atoms of the same elements but with a different amount of neutrons. This leads to small differences in mass and thus can affect their behaviour in physical and biological processes. However, the amount of neutrons does not affect the chemical properties of the element. An element can have several isotopes, but in general they can be categorised into stable and unstable isotopes. Hydrogen, the first element in the periodic table for example has seven isotopes, see Figure 1 (Holden et al., 2018). But only protium (1 electron, 1 proton) and deuterium (1 electron, 1 proton, 1 neutron) are stable isotopes (Sharp, 2007).

Whereas tritium and hydrogen isotopes with even more neutrons are not stable. Unstable isotopes are subject to radioactive decay with relatively short half-life times. In this thesis, the focus lies on stable isotopes. Furthermore, generally one of the isotopes is significantly more abundant in nature. In case of hydrogen, protium makes up 99.985% of all hydrogen, whereas deuterium only amounts to 0.015%, thus is quite rare (Sharp, 2007). One way of describing the ratio of lighter and heavier isotopes is the delta value in per mill (‰), i.e. δ^2H for hydrogen isotopes. Here, the ratio of the heavier isotope divided by the lighter (often more abundant) isotope is compared to their ratio within a standard, see also Eq. 1 in Chapter 3.7 (Sharp, 2007).

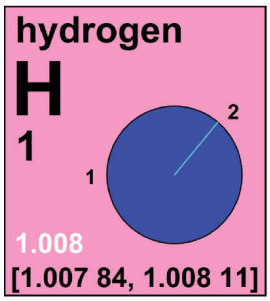

Stable isotope	Relative atomic mass	Mole fraction
^{1}H	1.007 825 0322	[0.999 72, 0.999 99]
^{2}H	2.014 101 7781	[0.000 01, 0.000 28]

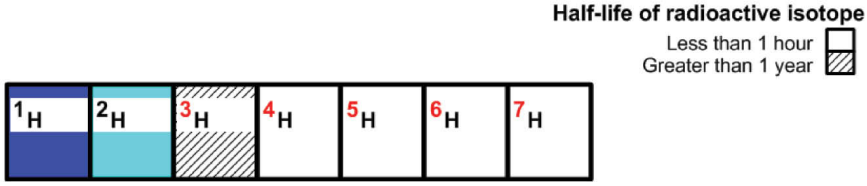

Figure 1: Isotopes of hydrogen, their stability, relative mass and abundance from: Holden et al., 2018.

Biochemical and environmental processes can lead to changes in the isotope ratio, e.g. by fractionation of heavier and lighter isotopes. The amount of fractionation does depend on several factors. Isotopes of elements with a low atomic mass generally fractionate more, because the relative mass difference of an additional neutron is greater. The fractionation is also increased if the natural abundance ratio is large. If the mass difference between two isotopologues is small, fractionation processes have no "preference" for one or the other. Thus, both isotopologues are used more equally, and the fractionation is dampened. Fractionation can happen because of the kinetic or the equilibrium isotope effects.

The kinetic isotope effect is usually much larger, compared to the equilibrium effect. Furthermore, kinetic fractionation happens in incomplete and unidirectional processes like evaporation or condensation (Sharp, 2007). For example, water molecules with lighter protium evaporates faster leading to clouds with more lighter hydrogen isotopes and thus depleted $\delta^2 H$ values compared to the source water. During condensation the opposite is the case, leading to more heavier isotopes in rainwater with enriched $\delta^2 H$ values (Sharp, 2007). The reservoir, in this case the clouds, therefore are becoming lighter during the transport from the sea inland towards the centre of the continent.

The equilibrium isotope effect can be seen as the effect of atomic mass on bond energy, with heavier isotopes forming stronger connections (Sharp, 2007). The effect is most importantly dependent on temperature and follows the relationship of $1/T^2$ (T in kelvin). This leads to a larger fractionation at cooler temperatures. In the case of the calcite-water equilibrium oxygen isotope fractionation, the fractionation at 25°C is 28.8‰, whereas at 600°C it is only 1‰(Sharp, 2007).

1.2.2 Usage of isotopes

Isotopes have proven to be useful in natural sciences as proxy indicators for e.g. paleo-climate research (Leng & Marshall, 2004). Depending on where a water sample with their respective δ^2H and $\delta^{18}O$ values plots on the global meteoric water line, an estimation on the source region and the climate (humid/arid) can be made (Xi, 2014). Other applications are the ^{14}C measurement of biological matter to calculate an approximate age of the sample (Kutschera & Rom, 2000) or the isotope analysis of tree rings to acquire a sense of climatic conditions during the lifetime of the tree (Saurer et al., 1997). The options are countless and with ongoing scientific advancements in methodology, these methods can be used for new applications (Schuler et al., 2021).

Stable isotopes of carbon and oxygen in plant carbohydrates (e.g. sugars, starch, tree-ring cellulose) have been used extensively as climate and plant physiological proxies and reliable high-throughput methods have been established (Boettger et al., 2007; Lehmann, Egli, et al., 2020; Richter et al., 2009; Saurer et al., 1997; Tcherkez et al., 2011; Xia et al., 2020). In contrast, hydrogen isotope ratios (δ^2H) have not yet been widely used. And if they were, mostly for cellulose samples and not for starch and sugars (Xia et al., 2020).

The exchangeable hydrogen problem

One main reason for the reduced application of hydrogen isotopes in plants is the lack of a reliable high-throughput method to measure δ^2H in non-structural carbohydrates (NSC, i.e. sugars & starch) and structural carbohydrates (i.e. cellulose). Most publications concerning hydrogen isotopes in plants focus on the water in different parts of a plant. Measuring the δ^2H of a given water sample is relatively easy with a well established method (Kelly et al., 2001). Water only consists of hydrogen and oxygen atoms, whereas in NSC carbon is also present, see Figure 2.

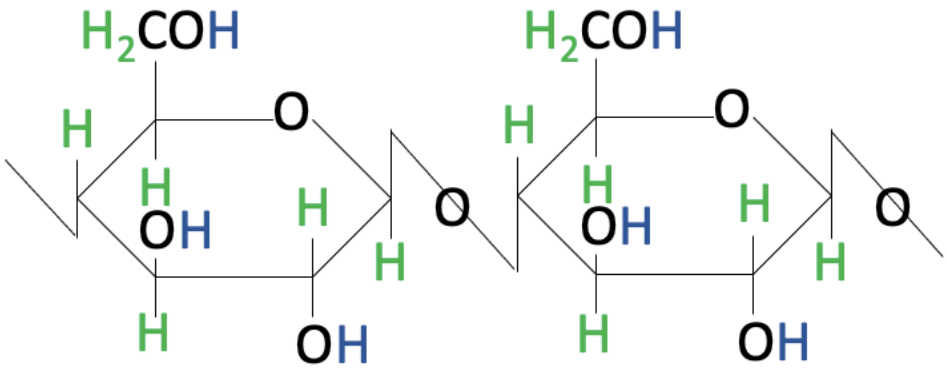

Figure 2: Structure of cellulose molecules. Hydrogen atoms bonded to carbon atoms indicated with green, and to oxygen with blue (modified from Rodriguez-Celis et al., 2017).

The cellulose structure has two distinct types of hydrogen bonds, concerning the ability of isotope exchange. Hydrogen atoms, that are bonded to carbon (green) and others, that are bonded to e.g. oxygen (blue). These bonds are not equal, since the C-H bond is thought to be stable ($H_{non-exchangeable}$, short H_{ne}), whereas the hydrogen bonded to oxygen can undergo isotope exchange with hydrogen of surrounding water or vapour ($H_{exchangeable}$) (Hobson & Wassenaar, 2018; Roden & Ehleringer, 2000; Schuler et al., 2021). Thus, leading to a possible strong alteration of the true potential environmental and metabolic information, that is only

stored in δ^2H_{ne}. However, this poses a problem for the mass spectrometer analysis. Since there, all hydrogen atoms are measured. So far, this was circumvented by the usage of site-specific natural isotope fractionation nuclear magnetic resonance spectroscopy (NMR) or nitration of cellulose to nitrocellulose (removing the hydroxyl hydrogen groups) before isotope ratio mass spectrometry (IRMS) (Roden & Ehleringer, 2000; Schuler et al., 2021). But these methods are highly labour intensive and the production of explosive compounds poses a health risk.

1.2.3 New equilibration method

A new approach was recently published by Schuler et al., 2021 using vapour-equilibration of the samples with two different water vapours with known δ^2H values. The exchangeable hydrogen is taking over the signal from the water vapour and thus, δ^2H_{ne} of NSC can be calculated with this high throughput method and without the production of dangerous compounds (Schuler et al., 2021).

Because the research done on NSC is so scars, this causes a major gap in the understanding of the different processes involved in ^2H fractionation. Hydrogen isotopes in plant material undergo strong photosynthetic and post-photosynthetic fractionation, which potentially holds crucial information concerning the photosynthetic and water-related features of plants (Sanchez-Bragado et al., 2019). Determining δ^2H of NSC could help to better understand the isotopic signal transfer from δ^2H of source and leaf water to δ^2H_{ne} of leaf (and tree-ring) cellulose and its variation with environmental changes such as temperature and humidity. Thus, $\delta^2H_{(ne)}$ could be used as a proxy for plant performance (Sanchez-Bragado et al., 2019).

1.3 Photosynthesis

Plants are using water, CO_2 and sun light to convert light energy to chemical energy for the production of organic compounds (Singhal et al., 1999). The photosynthetic process can be divided into two parts. In the "light" reaction, water molecules are split up into oxygen, electrons and protons using sun light energy (Johnson, 2016). In a next step these electrons and protons are used to reduce CO_2 to carbohydrates in the "dark" reaction (Calvin–cycle). The source materials enter the plant in different locations and ways. The water is taken up via the roots, CO_2 enters the leaf through small openings in the leaf called stomata.

1.3.1 Hydrological processes in plants

Water is supplied to the plants by precipitation and percolates into the soil. The roots can take up the water directly (mostly rainwater), or they might also reach the ground water, which could have a different isotopic composition (mixture of different rain events and affected by evaporation) (Zarebanadkouki et al., 2019). The water is then transported up to the leaves via the xylem (Zarebanadkouki et al., 2019). When the plant has access to enough water the leaves are hydrated and the stomata are fully opened (Johnson, 2016). However, if water is limited, the turgor pressure drops and the stomata are closed. This limits the loss of water through the stomata via evaporation.

The fractionation process can affect several points during this process. First of all, δ^2H of source water depends on the origin of the rain (water vapour source). The δ^2H of rain water is becoming more depleted with higher latitude, longer transport and altitude (Vreča & Kern, 2020). However, evaporation from the soil leads to enrichment of ^2H as it favours lighter water. If water percolates to deeper soil layers, it mixes with water from past rain events and ground water, which affect the isotopic composition. The evaporation effect is becoming smaller further from the surface. During plant water uptake through the roots, isotopic fractionation

is generally assumed to be insignificant, so that the δ^2H xylem water reflects the source water. Some exceptions have been observed, however, in halophytic and xerophytic species (Barbeta et al., 2018). When the water has reached the leaf, a ^{2}H enrichment can be observed because of the evapotranspiration favouring lighter water, which depends on the evaporative environment of the plant (Cormier et al., 2018).

1.3.2 Carbon fixation

C3

Once the CO_2 has entered the leaf, it is fixed into carbohydrates with the use of ATP and NADPH (produced during light reaction) in the Calvin cycle (Johnson, 2016). The product of the Calvin-cycle is glyceraldehyde 3-phosphate (GAP, a 3C sugar) which can then be converted into amino acids, lipids or sugars e.g. glucose. Glucose can then be stored as a polymer (starch) and or later be used for cellulose synthesis (Li et al., 2014). Plants using this pathway are usually called C_3 plants because of the main product being GAP (Johnson, 2016).

The actual incorporation of CO_2 is made by one enzyme (Rubisco) via a carboxylation reaction. However, Rubisco can also catalyse the fixation of oxygen via photorespiration (Singhal et al., 1999). This competes directly with the carboxylation by consuming ATP and thus represents an energy loss for the plant (Johnson, 2016). Photorespiration is much less favourable compared to the fixation of CO_2. However, the concentration of O_2 in the leaf is about 25 times higher than the CO_2 concentration (Johnson, 2016). So that the photorespiration can have a major effect.

C4

Some plants have evolved different methods to counter photorespiration by using CO_2 concentrating mechanisms (CCMs), see Figure 3. CCMs try to increase the CO_2 concentration within the leaf in close proximity to Rubisco. One such CCM is used by C_4 photosynthesis. C_4 plants possess a specialised organ (Kranz anatomy), with mesophyll cells rich in the enzyme phosphoenolpyruvate (PEP) carboxylase. PEP fixes CO_2 into 4C carboxylic acid (oxaloaceatate), which is then reduced by NADPH to malate (also a 4C acid), thus the name C_4 pathway (Johnson, 2016; Singhal et al., 1999). Then the malate is decarboxylated to pyruvate, which regenerates the NADPH and CO_2 in turn, which can then be efficiently used by Rubisco because it is so concentrated in the Kranz sheath cells (Johnson, 2016).

CAM

Another CCM is used by CAM plants. As mentioned above, CO_2 enters the leaves via the stomata. However, in dry and hot environments the stomata are closed during most of the day to avoid water loss. Therefore, the CO_2 concentration is low within the leaf and C_3 photosynthesis is not possible (Johnson, 2016). These plants fix CO_2 during the night, the CO_2 is catalysed by PEP carboxylase to malate and then stored in the vacuole (Johnson, 2016; Singhal et al., 1999). During the day, when the stomata are closed, malate is released and decarboxylated to CO_2 and pyruvate, which is then used by Rubisco in the Calvin-cycle (Singhal et al., 1999). The process is called crassulacean acid metabolism (CAM).

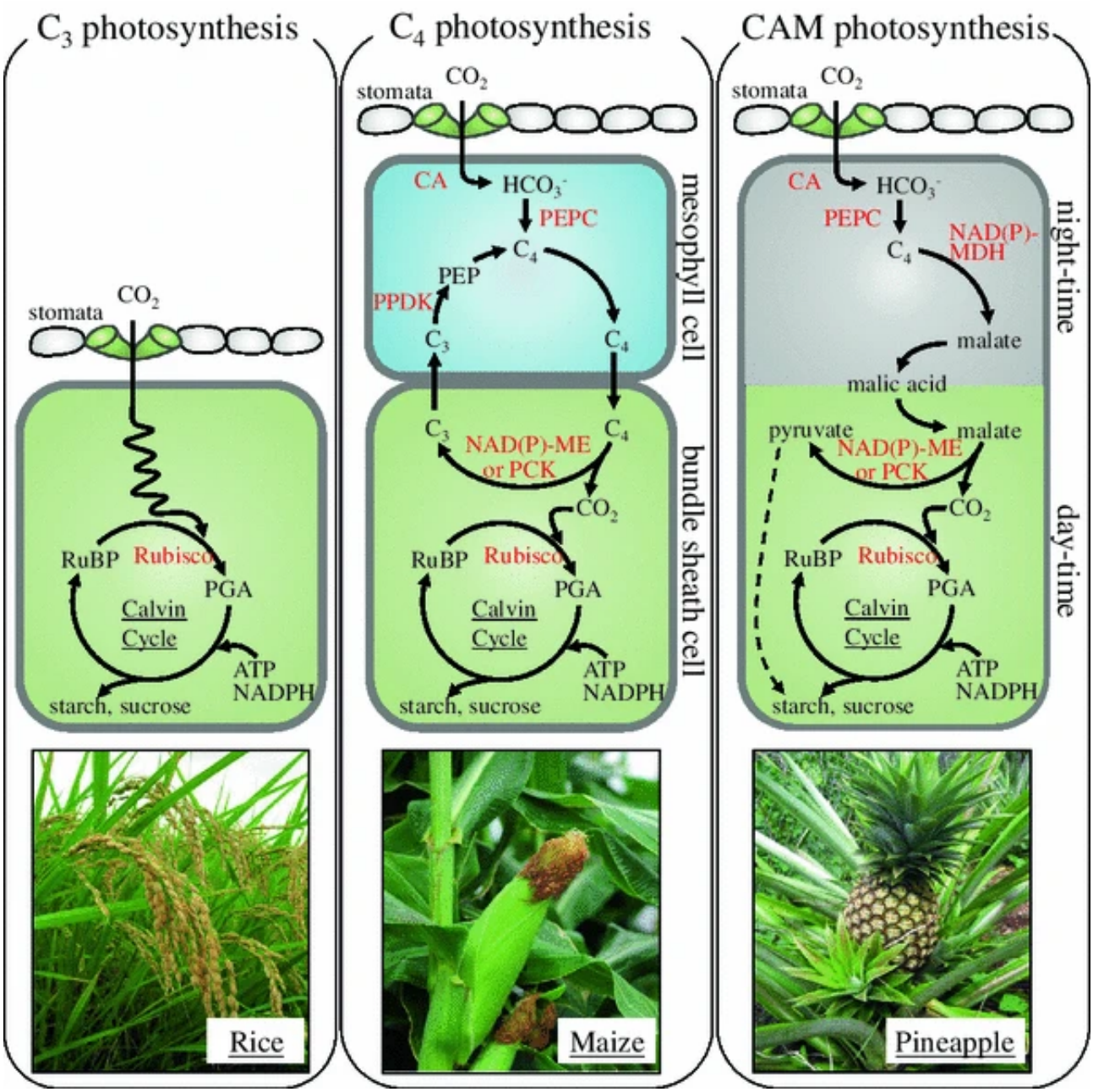

Figure 3: Shows the three carbon fixation pathways (C_3, C_4 and CAM) with one typical example organism (Source: Yamori et al., 2013).

Pathway of hydrogen isotopes in carbon fixation

When the water has made its way from the soil to the leaf of the plant, it is split up in the light reaction of the photosynthesis, producing e.g. NADPH and later the primary photosynthates (i.e. sugars). Luo et al., 1991 suggest that these early photosynthates are depleted of ^{2}H because of the fact, that NADPH is derived from hydrolysis reactions, strongly favouring lighter hydrogen.

Furthermore, these sugars can then fractionate further or interact with the surrounding leaf water (enriched in ^{2}H), thus increasing the δ^2H of starch and cellulose later on (Schuler et al., 2021). Additionally, sugars can be transported from autotrophic to heterotrophic tissue, inducing further ^{2}H enrichment in the tree-ring cellulose and carbon storage pools of the plant (Furze et al., 2018).

Moreover, the carbon fixation pathway has also shown to influence ^{2}H ratios in cellulose, with large differences in compounds between C_3, C_4, and CAM plants (Schmidt et al., 2003; Schuler et al., 2021; Sternberg et al., 1984). Liu et al., 2016 suggested, that δ^2H of leaf wax is differing between monocotyledons and dicotyledons, so this might also play a role in the hydrogen composition of the different plant compounds. However, the exact relationships and factors are not yet understood. This is why I will also compare monocots and dicots within the same carbon fixation type.

An interesting approach of looking at fractionation between different compounds is the biological fractionation factor (ϵbio). Cormier et al., 2018 describes the bio synthetic fractionation as one of three main influencing factors of δ^2H compositions. The other two being the water source and the evaporative environment. The ϵbio describes the general relationship between a product and its substrate, e.g. organic compounds being built within the leaf water environment ($\delta^2H_{organic}$ - δ^2H_{water}). In my specific case, I will be using two versions of ϵbio. The first being the fractionation of hydrogen between sugars and leaf water (δ^2H_{sugar} - δ^2H_{water} = ϵbioHA) in a autotrophic environment (production of primary assimilates). The second one being the fractionation factor between cellulose and sugars ($\delta^2H_{cellulose}$ - δ^2H_{sugars} = ϵbioHE) in a heterotrophic environment (usage of primary assimilates).

In general, carbon and oxygen stable isotopes have been well understood in terms of plant performance, with ^{13}C and ^{18}O of plant compounds reflecting transpirative and photosynthetic conditions (Sanchez-Bragado et al., 2019). And it has been suggested that also ^{2}H composition can be used to gain a deeper understanding of plant performance under different environmental conditions (temperature, humidity).

1.4 Temperature effects

Different plant species growing in various parts and climatic regions have their optimal growth temperature on which they are able to reach the best photosynthetic performance. For example CAM plants adapted their carbon fixation pathway to survive a dry and hot environment (Johnson, 2016). And it makes sense, that these plants have a higher temperature optimum. In contrast, C_3 plants might start to close their stomata with increasing temperature, which affects evaporation and thus δ^2H composition. A study by Buhay et al., 1996 shows a temperature dependent effect of hydrogen stable isotopes in plants, which is opposing the evaporative enrichment effect. Furthermore, hydrogen fractionation during cellulose synthesis can be strongly influenced by temperature (DeNiro & Epstein, 1981). But, it was shown that these effects are also species specific. Additionally, in tree-rings only δ^{18}O correlates well with climatic conditions and δ^2H does not, even though hydrogen and oxygen are usually tightly linked (Lehmann, Vitali, et al., 2020). This might be due to difference in autotrophic and heterotrophic processes. Therefe, I will analyse how large the species specific fractionation effects are and how they compare between carbon fixation pathways.

1.5 VPD effects

Stomata closure is not only a reaction of increasing temperature, but is also affected by the air humidity (Merilo et al., 2017). With an increase in temperature comes an increase of saturation vapour pressure (how much moisture the air can hold). However, the actual vapour pressure does not increase equally to the saturation vapour pressure, thus leading to a vapour pressure deficit (VPD, i.e. the difference between saturated and actual vapour pressure)(Grossiord et al., 2020). VPD is seen as one of the major environmental factors affecting the stomatal conductance and thus photosynthetic activity (Inoue et al., 2021). Rising VPD is leading to

stomatal closure and ramp down of photosynthesis (Grossiord et al., 2020). Thus, if the ^{2}H composition can indeed be used as a proxy for plant performance, this should be visible in the ^{2}H composition. The effects of VPD, however, might be different compared to the temperature effects. Thus both are being tested separately.

Chapter 2

Hypothesis

In this thesis, I want to investigate how environmental factors (e.g. temperature, vapour pressure deficit (VPD) and carbon fixation pathways influence the δ^2H of leaf water, leaf sugar, and leaf cellulose applying a newly developed analytical method (Schuler et al., 2021). The goal is to reach a deeper understanding of the mechanisms and drivers of ^2H fractionation in plant leaves of different photosynthetic pathways:

- I expect an enrichment of ^2H in the leaf water with higher temperatures and increased VPD, especially in C_4 plants, because of the higher temperature optimum (Leaney et al., 1985; Sanchez-Bragado et al., 2019; Yamori et al., 2013).

- The sugars in turn will be depleted in ^2H of C_3 plants compared to the leaf water, because the hydrogen ions used in NADPH formation are already depleted (Luo & Sternberg, 1991).

- The cellulose might be slightly enriched compared to the sugars because of the hydrogen exchange in the enriched leaf water (Yamori et al., 2013).

- The VPD effect likely only affects the leaf water and thus the sugars, but will not lead to further fractionation during cellulose synthesis (constant ϵbioHE) (Cormier et al., 2018).

- Additionally, I expect large differences in δ^2H between C_3, C_4 and CAM plants due to strong differences in plant physiology with C_4 and CAM showing an enriched ^2H composition, compared to C_3 plants (Leaney et al., 1985).

- And plants with crassulacean acid metabolism (CAM) likely exhibit no temperature and VPD effect, since the main gas exchange happens at night (Black & Osmond, 2003).

Chapter 3

Methods

3.1 Experimental Setup

Different plant species with C_3 (n=16), C_4 (n=9) and CAM (n=13) carbon fixation pathways were grown in walk-in climate chambers at WSL Birmensdorf, as part of the PhD project of Philipp Schuler. The plants were grown under three climatic conditions with at least three replicates per species. The climate chambers were programmed to 16 daytime hours and 8 nighttime hours with constant conditions (Table 1). The lighting consisted of uniform fluorescent tubes (OSRAM L 36 W 777 Fluora, Osram Licht AG, Munich, Germany) with a photosynthetically active radiation (PAR) of 110µmol m^{-2} s^{-1} at plant height. C_3 and C_4 plants were watered 2-3 times per week up to field capacity with regular tap water ($\delta^2H = 79.9 \pm 2.4$ ‰) during the whole experiment (Schuler et al., 2021). CAM plants were watered 1-2 times per week to prevent complete dehydration of the soil.

Table 1: Climate chamber conditions during the day (variable, the three climatic conditions that are being tested) and night (constant).

Temperature [°C]	**VPD**	**air VPD** [kPa]	**RH** [%]	
20	low	1.18	50	Daytime (16hrs)
30	low	1.29	70	
30	high	2.59	40	
15	-	0.69	60	Nighttime (8hrs)

For this thesis, I selected 10 x C_3, 7 x C_4 and 8 x CAM species (with 3 replicates each) for each of the three conditions. This resulted in 225 samples that needed to be processed. The amount of species per carbon fixation type is not balanced because for the C_3 group more species were added to achieve a balanced data set for the comparison of monocotyl and dicotyl plants. Furthermore, one more CAM species was added as a buffer, since for some CAM species parts of the extraction proved difficult in test runs and we expected not all of the CAM species to be obligatory CAM (Winter et al., 2008). At last, the seven C_4 plants make up all the available C_4 species. All selected species are shown in Table 2 below. The δ^2H in leaf water, purified sugars (NSC) and cellulose was measured for each plant sample.

Table 2: Shows the selected plant species. The carbon fixation pathway is shown in the column "Type", the column "Cot." indicates whether the species belongs to the monocotyledons or dicotyledons.

	Species	**Type**	**Cot.**
1	*Quercus pupescens - L.*	C3	Dicot
2	*Oryza sativa - L.*	C3	Mono
3	*Hordeum vulgare - L.*	C3	Mono
4	*Salvia hispanica - L.*	C3	Dicot
5	*Begonia semperflorens - HORT.*	C3	Dicot
6	*Begonia maculata - Raddi*	C3	Dicot
7	*Anthurium sp. - Schott*	C3	Mono
8	*Cyperus sp. - L.*	C3	Mono
9	*Abelmoschus esculentus - Moensch (L.)*	C3	Dicot
10	*Zantedeschia aethiopica - Spreng. (L.)*	C3	Mono
1	*Zea mays - L.*	C4	Mono
2	*Pennisetum glaucum - Morrone (L.)*	C4	Mono
3	*Sorghum bicolor - Moensch (L.)*	C4	Mono
4	*Amaranthus caudatus - L.*	C4	Dicot
5	*Amaranthus tricolor - L.*	C4	Dicot
6	*Salsola soda - L.*	C4	Dicot
7	*Setaria italica - P. Beauvois (L.)*	C4	Mono
1	*Phalaenopsis - Blume*	CAM	Mono
2	*Delosperma cooperi - L. Bolus (Hook.f.)*	CAM	Dicot
3	*Rhipsalis sp. - Gaertn.*	CAM	Dicot
4	*Hylocereus sp.*	CAM	Dicot
5	*Sedum sp. - L.*	CAM	Dicot
6	*Senecio sempervivus - Sch.Bip.*	CAM	Dicot
7	*Aptenia cordifolia - Schwantes (L.f.)*	CAM	Dicot
8	*Euphorbia pulcherrima - Willd. ex Klotzsch*	CAM	Dicot

3.2 Sampling

The plant leaves were sampled in the early afternoon, to assure sufficient sugar production and therefore availability for the further purification steps (Cernusak et al., 2015). The leaves were cut off, pushed into glass exetainer vials (Exetainer, Labco, Lampeter, UK, Prod. No. 738W), stored on ice for max. two hours and then placed into a freezer (-20°C) immediately after sampling, to stop further biological processes and thus unwanted isotope fractionation. The vials were filled as much as possible to ensure that there is enough biomass for all purification steps. This is especially important for CAM plants, since the thick leaves have a high relative water content and after the water extraction the available biomass for sugar and cellulose extraction is smaller compared to other carbon fixation types.

3.3 Leaf water

3.3.1 Water extraction procedure

The water extraction was done with a cryogenic vacuum distillation according to West et al., 2006, see Figure 4. First, the water bath was turned on and heated to 80°C. This not only stops potential biological processes and thus further isotope fractionation, but also assures a faster evaporation of water inside the sample vial. Deionized water should be used as to prevent chalk buildup in the basin. The basin was then covered with a lid to reduce evaporation and risk of sample loss, when working over the water bath. But this also minimises the amount of water vapour that could enter into the tubing while the samples are not yet connected to it.

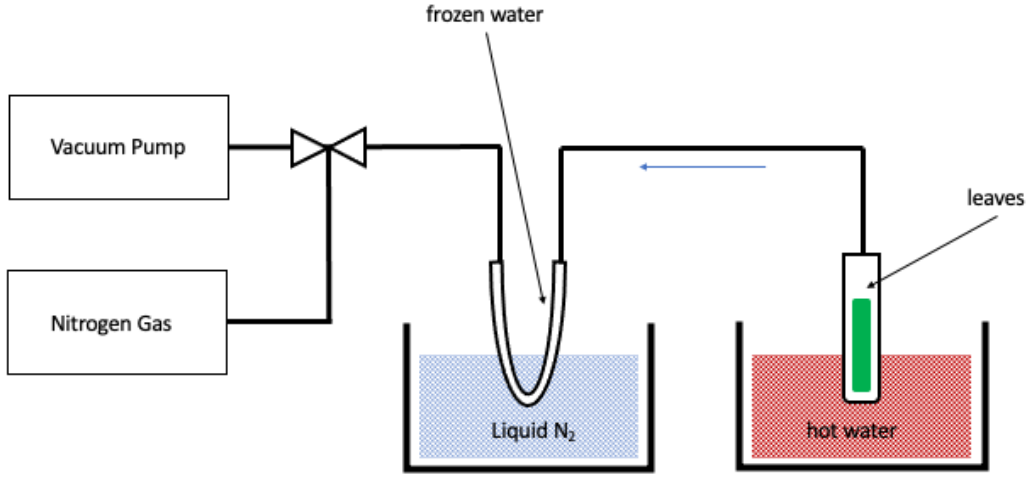

Figure 4: Simplified diagram of cryogenic vacuum distillation. The samples are places in the hot water bath (red) and the u-tube in liquid nitrogen (blue). Then the vacuum is applied leading to the evaporation of water from the sample to depositing and freezing in the u-tube. The system is then flushed with nitrogen gas and the extracted water as well as the dried sample can then be collected.

Then, the samples were taken out of the freezer and brought in order. For soil samples, a layer of glass wool or a filter should be added to prevent dust in the lines. I have also found that a filter can be beneficial in leaf samples to keep the sample inside the glass vial during initial vacuum creation. Thick leaves and fully filled sample vials are especially susceptible for this. In the later case it can also help to make a small hole with a needle through the sample to the tube bottom. So the the evaporating water can escape freely. The usage of glass wool, however, is not advised when the sample is needed later on (in my case). Therefore, I only used filters (Carl Roth, Safe cone filter for 10ml Pipettes, Karlsruhe, Germany) for my samples.

Before connecting the actual sample tubes, the cooling traps were shortly purged with dry N_2 gas to flush out ambient air moisture. For this, the nitrogen bottle was opened and the pressure was adjusted to around 1 bar. The pressure can stay the same for the rest of the extraction, but should not be higher, so the glass tubing and vials do not break.

Then the buckets were filled with liquid nitrogen and placed under the cooling traps. Furthermore, the cover of the water bath was also removed and the lines were lowered slowly into the liquid nitrogen and water respectively. When the liquid nitrogen had stopped boiling, the vacuum was applied slowly. This way the sample is not sucked through the tubing into the cooling trap. When a vacuum of $< 5.0 * 10^{-2}$ mbar is reached the valve can be closed again. This step is repeated for the next five lines until all of the lines are under vacuum. Then all the valves can be opened. If one of the sets is leaking this is immediately recognisable, which makes troubleshooting easier and does not compromise the other samples. The lines should always be inside the liquid nitrogen when the vacuum valve is open. Otherwise part of the sample might be lost and also the moisture can damage the vacuum pump.

The samples were then extracted for two hours. During this time the water and liquid nitrogen levels were checked regularly. Then, the vacuum pump and the water bath were turned off. The nitrogen gas was applied to equalise the internal pressure of the lines and to not let ambient moisture inside the system. The samples were then disconnected from the lines and directly covered with the respective lids. Afterwards, the cooling traps were disconnected and the openings were covered with rubber stoppers to avoid evaporation during the melting process.

When the water inside the cooling traps was fully melted, it was pipetted into 2ml gas-chromatography (GC) glass vials (if there was only a small amount vials with 350 µl inlets were used. Additionally, the samples were filtered (0.45µm nylon filter, Infochroma AG, Zug, Prod No. 8813C-N-4), depending on the available volume and degree of pollution of the sample. The samples were then stored in the freezer at -20°C. Furthermore, the cooling traps were rinsed with deionized water and dried in the oven at up to 80°C.

3.4 Leaf sugar

3.4.1 Milling and Preparation

The dried samples were taken out of the glass vial, homogenised (with metal spatula or scissors) and filled into acrylic containers. Half of the sample was used for the extraction of water soluble non-structural carbohydrates (WSC) and the rest for the cellulose extraction. For the NSC the sample was finely powdered with a ball-mill (Retsch MM400, Retsch, Haan, Germany). For smaller samples, metal tubes with small metal beads were used. In this case, less sample is lost. Then 100mg powdered sample was weighed into 2ml screw cap tubes, which were then labelled on the cap, as well as on the side. No tape or stickers should be use as the tubes might stick to the thermo shaker later on.

3.4.2 Hot water extraction of water-soluble compounds (WSC)

The WSC extraction was done according to the modified protocol of Lehmann et al., 2017. Around 500ml of Milli-Q water in an Erlenmeyer beaker was heated to 85°C in a water bath and the thermo-shaker plate (Thermal Shake lite, VWR, Leuven) was also heated to 85°C. Then 1.75ml of the hot Milli-Q water was pipetted into the sample tube (2x 850 µl while vortexing in between). The hot water improves the extraction and dissolution of WSC in the water and also inhibits enzyme activity. When the sample powder was fully suspended the tubes were place inside the thermo-shaker for 30 minutes.

Then the sample tubes were places in a rack and let cool for about 5 minutes. The tubes were then centrifuged (Centrifuge 5415 R, Eppendorf AG, Hamburg) for 2 minutes , 12'000 g at room temperature (RT, 25°C). The supernatant (WSC) was then pipetted into 2ml Eppendorf tubes. The supernatant as well as the remaining pellet were stored at -20°C. The pellet could be used for further starch or cellulose extraction (see 3.5.2).

3.4.3 Purification of WSC

Preparation and conditioning of cartridges

First, the vacuum extraction system needs to be set up. For this, the waste tray was inserted in the glass container and the vacuum pump was connected. Before adding the cartridges, the valves of the Luer-locks connectors were turned into the closed position. Then the OnGuard cartridges were assembled from top-to-bottom: Black (Dionex OnGuard^{TM} II H, Thermo Fisher Scientific, Karlsruhe, Prod No. 057085), Yellow (Dionex OnGuard^{TM} II A, Thermo Fisher Scientific, Karlsruhe, Prod No. 057091), White (Dionex OnGuard^{TM} II P, Thermo Fisher Scientific, Karlsruhe, Prod No. 057087), see Figure 5. The cartridges remove amino acids, organic acids and phenolic compounds. Furthermore, gloves were worn during this step to avoid contamination.

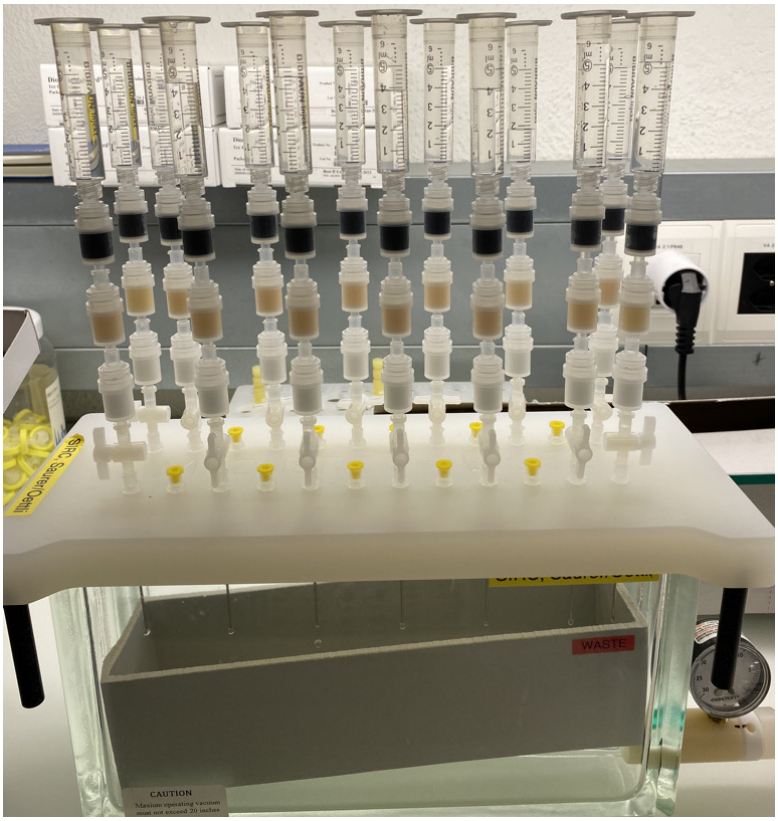

Figure 5: WSC purification vacuum system with different WSC samples added onto the column. Each tower consist of a syringe on the top, a black (H), yellow (A), white (P) cartridge in this order. The towers are place on top of the vacuum chamber and divided by the valve (Source: Oliver Rehmann, WSL Birmensdorf.

5ml syringes were filled with Milli-Q water and connected to the cartridge tower. The water was slowly pushed through while holding the tower upside down (syringe, H cartridge etc). This ensured that the cartridge filling is moistened equally and no air pockets remained, which might affect functionality. From now on the cartridges should never run dry. The cartridge tower was then connected to the vacuum extraction system. The syringe was disconnected and only the bottom part (without the plunger) was connected to the cartridges again. During this step, a water drop should remain on top of the black cartridge (air pockets). The syringes were then filled with another 5ml Milli-Q water each.

Afterwards, the vacuum pump was turned on (valves are still closed at this moment). The procedure works best with a vacuum around 15in Hg ($\sim$ 0 5bar). Higher vacuums could break the glass container. Depending on how familiar one is with the system, 2-3 cartridge towers can be opened at once and the water can percolate through. After only 1ml of the water remained in the syringe, the valves were closed and another 5ml was added. This procedure was then repeated for all cartridge towers and for a total amount of 30ml including the initial volume before adding the sample. In the last round, the valves were closed at a rest volume of 1ml remaining in the syringe.

Then all the valves were closed, the vacuum pump turned off and the waste tray was emptied. The insert for the 15ml Falcon tubes was filled with the labelled tubes and inserted into the vacuum chamber. When placing the lid on, it should be checked if all the metal tubes on the bottom actually go inside the falcon tubes. The tubes its self were first labelled (tube and lid) and then weighed in. Later on the difference between the initial weight and the finished weight will be used to calculated the amount of WSC gained and determines the concentration adjustment later on.

Loading cartridges with WSC

The WSC samples were then defrosted, strongly vortexed and subsequently centrifuged for 2 minutes, 12'000 g, at RT. The samples should not be left at room temperature for to long, as this can lead to oxygen isotope exchange with ambient water.

The samples were then added to the columns with the vacuum on. When the sample was almost fully infiltrated, 1ml of Milli-Q was added. An additional 1ml and 2 x 2ml were then added in the same way to elude the sugars from the cartridges. When there was around 7-8ml of sample water mixture in the falcon tube, the valve of the columns was left open and the cartridges were able to run dry. Theses steps were then repeated for all of the columns. Then the vacuum was released slowly from the side of the vacuum pump, as opening the cartridge valve could have lead to spillage during the sudden airflow and therefore loss of sample. The Falcon tubes were then be placed back into the freezer (-20°C) for at least 24 hours.

3.4.4 Sugar preparation for analysis

Freeze drying

The frozen Falcon tubes with the sample water mixture were taken out of the freezer and parafilm (Parafilm "M", Bemis, USA. Prod. No. NEENAH WI 54956) was added on top. Small holes were made with a needle and they were subsequently placed in the freezer again for another 2 hours. The tube lids were placed in a box in the same order as the samples.

The freeze dryer (LSL SECFROID, Aclens) was cooled down for 1-2 hours until a internal temperature of -50°C was reached. Then the samples were placed inside the vacuum chamber and the vacuum pump was turned on. The drying process was running for 3-4 days (depending on the amount of samples and liquid) at a vacuum of -0.8bar. The now dry WSC samples were then taken out of the freeze dryer and immediately closed with their respective lids. They were then weighed out and stored at room temperature.

Filling samples in capsules

Silver foil capsules (5.5 x 9mm, IVA Analysentechnik GmbH & Co. KG, Germany, Prod. No. SA76981106) were then used for the analysis of the samples. For this purpose, the weight of WSC was calculated by subtracting the initial weight of the tube from the end weight including the WSC. Depending on the amount of WSC available, different concentrations of the samples were made by adding 1ml, 500µl or 250µl of Milli-Q water. Samples were then vortexed until the WSC were fully dissolved. The silver capsules have a volume of a maximum of 130µl. So the concentrations were adjusted, that with one injection of a maximum of 130µl a sample weight of 1mg would be reached in each silver capsule. The capsules itself were weighed in when empty and placed inside a 96 well plate and then injected with the samples. Afterwards, the plates were frozen and freeze dried for two days, similarly to the Falcon tubes above (see 3.4.4). Capsules where then weighed out and the sample weight inside each capsule was calculated.

Because the WSC weight from the Falcon tubes are not always exact, capsules with a sample weight under 750µg were injected and freeze dried again. Depending on the sample the drying procedure can lead to small holes in the capsule, in this case, a new capsule was used and the first one was folded and placed inside the second capsule.

During the equilibration (see 3.6.1) of the samples later on, the sugars can melt and could leak out of the capsule. Therefore, each capsule was folded into a ball and placed inside an new empty silver capsule of the same size. Which was then also folded and placed back inside the 96 well plate. Furthermore, two sets of all the samples are needed for the hot water vapour

equilibration and therefore two capsules per samples were injected and prepared as described above. The samples where then stored inside a desiccator until measurement.

3.5 Leaf cellulose

The rest of homogenised leaf samples were then used for the extraction of cellulose. Samples with enough biomass (100mg or more) were extracted in F57 fibre filter bags (polyester and polyethylene with an effective pore size of 25 µm; ANKOM Technology, Macedon NY, U.S.A. (Schuler et al., 2021)). However, for some samples there was not enough biomass available for this kind of cellulose extraction. In this case, the cellulose extraction was made in the Eppendorf tubes used earlier in the NSC extraction (see 3.4.2). Both the in-tube and the filter bag extractions were performed inside a fume hood.

The sample was filled into the filter bags (100mg) and the bags were then heat sealed as close to the sample as possible. The top of the bag was cut max. 1cm above the seal line and a binary code was then cut into this part (0 = V-cut, 1 = I-cut). The physical binary code is necessary because the bleaching step would erase other markings. The code is read from left to right and to indicate the right orientation one edge of the bag was cut off (cut side always on the left = right side up). Since only about 50 bags can fit inside the soxhlet insert, the same binary code shows up several times. The samples were therefore additionally colour coded and extracted in individual groups.

3.5.1 Sample cleaning

Soxhlet purification

The soxhlet extraction was done to remove the bulk of lipids from the beginning and modified from Gaudinski et al., 2005. The bagged samples were added to the soxhlet apparatus in sets of 50 and a 2:1 Toluene:Ethanol mixture was used for the extraction (Toluene ROTISOLV HPLC, Roth, Karlsruhe, Prod. No. 7346.1; Ethanol , Fluka, Hungary, Prod. No. 11809107). A sacrificial filter bag was placed on top of the samples to avoid physical erosion of the sample bags. Since the temperature for the extraction was not mentioned in Gaudinski et al., 2005, I started with a low temperature and began increasing the temperature slowly over 30 minutes, to not risk boiling retardation. Additionally, five zeolite stones were added with each new batch of solvent. A infrared measurement showed a boiling point of 74.9°C (see Figure 6). The solvent was changed after each set of samples.

Gaudinski et al., 2005 recommends to run the extraction for 24 hours. However, I was not allowed to let the extraction run over night for safety reasons. The soxhlet extraction was therefore run over 2-3 days or until the solvent was clear in the top flask. Over night, the extraction was stopped so that the solvent was in the bottom flask and the samples were not submerged in the solvent.

After the Toluene:Ethanol solution was not becoming dark anymore, the inserts with the samples were taken out of condenser flask and left in a beaker to dry for 24 hours under the fume hood. Then the same procedure was repeated with just Ethanol as solvent. Afterwards the samples were dried over night in the oven at 60°C.

NaOH cleaning

In the second cleaning step the 5% Sodium hydroxide (NaOH, 50g per 1L deionized water) solution removes fats, resins, oils and tannins from the sample (NaOH $\geq$ 99%, Roth, Karlsruhe, Prod. No. 9356.3). Roughly 500ml of NaOH was needed for each Erlenmeyer flask (2 x 250ml).

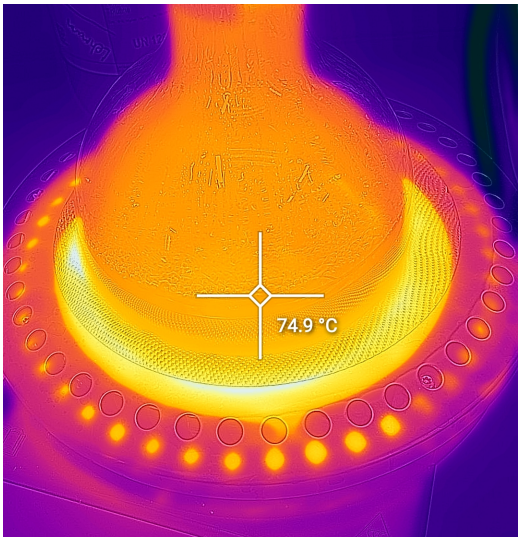

Figure 6: Flir infrared image of soxhlet bottom flask at boiling (Source: Oliver Rehmann, WSL Birmensdorf).

The samples were covered with the NaOH solution and left for two hours in the water bath at 60°C. Then the solution was poured directly into the corresponding recycling containers. This step was repeated for a second time and then the still wet samples were rinsed with boiling deionized water three times.

Bleaching

In this bleaching step the a solution of 7% Sodium chlorite ($NaClO_2$, 87,5g ($\sim$ 80% $NaClO_2$) in 1L deionized water) is mixed with 2-4ml of 96% acetic acid (CH_3COOH) until the pH of the solution is between 4-5 ($NaClO_2$ tech. nominally 80%, Alfa Aesar, Kandel, Prod. No. 231-836-6; Acetic acid ROTIPURAN 100%, Roth, Karlsruhe, Prod. No. 3738.5). The pH was measured with pH indicator strips. For each bleaching run 250ml of solution was filled into the Erlenmeyer flask and then placed in the water bath at 60°C (same as before). The solution then slowly reacted over the next $\sim$10 hours. The total extraction time can be roughly estimated as 30 hours per 10mg sample for smaller sample volumes. The process, however, is not linear and for my $\sim$100mg samples seven bleaching runs were performed. After each run, the solution was needed to be made from the start.

When the samples were fully bleached, they were rinsed three times with boiling deionized (DI) water, and squeezed to get rid of most of the moisture. Then the filter bags were taken out of the Erlenmeyer flasks and left on plates to dry in the oven over night (or at least four hours) at 60°C.

The bags were then be opened and the extracted cellulose was fill into weighed-in Eppendorf tubes. Since the sample inside the bag was not milled, the samples needed to be homogenised. For this, the tubes were filled with Milli-Q water and left to soak for two hours. Then each tube was treated with the sonic transducer to break the bonds in the sample. The now homogenised samples were then placed in the freezer over night and freeze dried for two days (see 3.4.4).

3.5.2 In-tube extraction

The in-tube extraction was done analogue to the bag extraction. But with the samples, that did have less than 100mg biomass. As a control, eight samples were extracted with both protocols (2x C_3, 2x C_4, and 4x CAM).

Toluene:Ethanol extraction

The pre-cleaning step with 2:1 Toluene:Ethanol was done by directly injecting 1ml of solvent into the Eppendorf tube with the sample pellet. Some glass pearls were added for better mixing. The samples were vortexed and placed in the heat-shaker plate at 60°C for 24 hours. Then the tubes were centrifuges for 2 minutes, 12'000 g, at RT and the supernatant was emptied into the corresponding recycling bin. The tubes were then left to dry over night in the initially hot but turned off heat plate. Just like in the bag extraction the same was repeated with just ethanol and dried again.

NaOH cleaning

Equal to the filter bag extraction the same NaOH solution was added to the Eppendorf tubes (∼1ml per Tube), vortexed and left for 2 hours at 60°C. The tubes were centrifuges for 2 minutes, 12'000 g, at RT and the NaOH solution was replaced once more. The sample in the tubes was then rinsed with boiling DI water, vortexed, centrifuged etc. for a total of three times.

Bleaching

Similarly, the same procedure as in the filter bag extraction was used by adding 1ml of the $NaClO_2$ solution to the tube. The tubes were then left in the heat shaker plate for 10 hours at 60°C. This bleaching was repeated for a total of seven runs. Just like before, the samples were then rinsed with deionized water three times. The tubes were then also filled with 1ml of Milli-Q water and treated with the ultrasonic transducer and freeze dried for two days.

3.5.3 Preparation for analysis

For the cellulose measurement, 1mg of sample was weighed into a 3.3 x 5 mm silver foil capsule (IVA, Prod. No. SA76980506) and tightly packet to form a ball. Similar to the preparation of the NSC samples the cellulose was also packed twice (one capsule for each of the two equilibration steps. However, since cellulose will not melt during this process, they were only packed in one capsule and not double as before.

3.6 Isotope Analysis

The isotope measurements were all performed at the central lab at WSL, Birmensdorf. The δ^2H of the water samples were analysed with a high temperature conversion elemental analyser, which was coupled to a DeltaPlus XP isotope ratio mass spectrometer (TC/EA-IRMS; Finnigan MAT, Bermen, Germany). The samples were calibrated with working standards D1-D5 ($\delta^2 H_{VSMOV}$).

3.6.1 Hot water vapour equilibration

For the sugar and cellulose measurements the hot water vapour equilibration method was used (Schuler et al., 2021). Both the sugar and cellulose samples were placed into the equilibration chamber with their respective standards. The first sample set was equilibrated with water 1 ($\delta^2 H = -160$ ‰) whereas for the second sample set water 2 ($\delta^2 H = -480$ ‰) was used. The water was pumped (1.7ml h^{-1}) into the hot equilibration chamber (130°C) for two hours and so that the water evaporates instantly. After the two hours the water flow was stoped and N_2 gas (N_2 5.0, PanGas AG, Dagmersellen, Switzerland, Prod No. 2220912) was fed into the still hot chamber at 1bar for two additional hours, to remove excess moisture.

The samples were then directly transferred to the Zero Blank Autosampler (N.C. Technologies S.r.l.) while still hot, that was connected to a sample port of a high-temperature elemental analyser system. The elemental analyser was coupled via a ConFlo III interface to a DeltaPlus XP IRMS (TC/EA-IRMS, Finnigan MAT, Bremen, Germany). The autosampler was then evacuated up to 0.01mbar and subsequently filled with dry helium gas to 1.5bar. The sample pyrolysation in the reactor was done following the paper by Gehre et al., 2004 with dry helium (150ml min^{-1}) as carrier gas to the IRMS.

The raw δ^2H values of the standard material and samples were offset corrected with a PEF standard (IAEA-CH-7 polyethylene foil (PEF; International Atomic Energy Agency, Vienna, Austria). Afterwards the $\delta^2 H_{ne}$ of the samples were normalised against $\delta^2 H_{ne}$ of Merck, Finnish and Russian sucrose for the NSC (Finish sucrose from 2019, Suomalainen Taloussokeri, Kantvik, Finland; Russian sucrose, household sugar from a Russian supermarket supplier). Whereas for the cellulose samples the corresponding nitrocellulose of the cellulose from Spain, Siberia and spruce (all in house standard) have been used next to PEF.

3.7 Calculations & Statistics

All isotope ratios were calculated with Eq. 1 according to Coplen, 2011. Were $R_{Sample} = {}^2H/{}^1H$ and $R_{Standard}$ = Vienna Standard Mean Ocean Water (VSMOV2). To convert to per mill (‰) values for δ the values were multiplied by a 1'000.

$$\delta = \frac{R_{Sample} - R_{Standard}}{R_{Standard}} \tag{1}$$

Furthermore, to calculate $\delta^2 H_{ne}$ the % portion of exchangeable hydrogen in the equilibration can be calculated with Eq. 2 (Filot et al., 2006). Here $\delta^2 H_{e1/2}$ are the $\delta^2 H$ values of the two equilibrations of the sample. Where as $\delta^2 H_{w1/2}$ represents the $\delta^2 H$ of the two waters use for the equilibration ($\delta^2 H_{w1} = -160$ ‰, $\delta^2 H_{w2} = -480$ ‰). Additionally, α_{e-w} is the fractionation factor and we use a value of 1.082 for both the NSC and cellulose samples (Filot et al., 2006) since both compounds have the same hydrogen bonds. The non-exchangeable fraction ($\delta^2 H_{ne}$) can be calculated with x_e and Eq. 3. In Eq. 3 only the values of one of the equilibrations is needed.

$$x_e = \frac{\delta^2 H_{e1} - \delta^2 H_{e2}}{\alpha_{e-w} * (\delta^2 H_{w1} - \delta^2 H_{w2})} \tag{2}$$

$$\delta^2 H_{ne} = \frac{\delta^2 H_{e1} - x_e * \alpha_{e-w} * \delta^2 H_{w1} - 1000 * x_e * (\alpha_{e-w} - 1)}{1 - x_e} \tag{3}$$

While the offset correction, normalisation and calculation of x_e and $\delta^2 H_{ne}$ were performed using Microsoft Excel. Further statistical analysis of the samples and the creation of figures was done using RStudio. Significant results are indicated with codes representing the p-value: '****' 0.0001 '***' 0.001 '**' 0.01 '*' 0.05 '.' 0.1 ' '. This is valid for the whole thesis.

Chapter 4

Results

4.1 Carbon fixation pathway comparison

In Figure 7 the differences between the plant compounds (water, sugar and cellulose) within the same carbon fixation types are shown. For the C_3 plants, all compounds are significantly different from each other (p-value < 0.0001) in the unpaired t.test. In C_4 and CAM plants, the same is true for the comparison of δ^2H water-cellulose and sugar-cellulose, but no significant difference can be observed between δ^2H water and δ^2H_{ne} sugar.

In C_3 plants, the sugar is depleted in ^{2}H compared to the δ^2H of water, and the δ^2H_{ne} cellulose is enriched compared to sugar and slightly depleted compared to water. Another trend is visible for C_4 plants, here the δ^2H water and δ^2H_{ne} of sugar are similar and the δ^2H_{ne} of cellulose is clearly enriched in ^{2}H. The results for CAM plant resembles the ones from C_4 plants, however, all compounds are slightly more enriched in ^{2}H compared to C_3 and C_4 plants. Furthermore, there is a steady increase of $\delta^2H_{(ne)}$ from water to sugar to cellulose.

The standard deviation (SD) is not equal in all compounds and there are also differences in between carbon fixation pathways, see Table 3. In C_4 plants for example, the SD is between 12.6 and 13.8‰ when comparing the different compounds. Similar values are observed in the SD δ^2H water of C_3 and CAM plants with 14.8 and 15.6‰, respectively. The SD of C_3 cellulose could also fit in the same group, although a bit higher with a value of 18.1 ‰. A clear difference in variation is visible in C_3 sugar and CAM sugar and both cellulose. Here the SD is much larger (36.7 - 55.4‰).

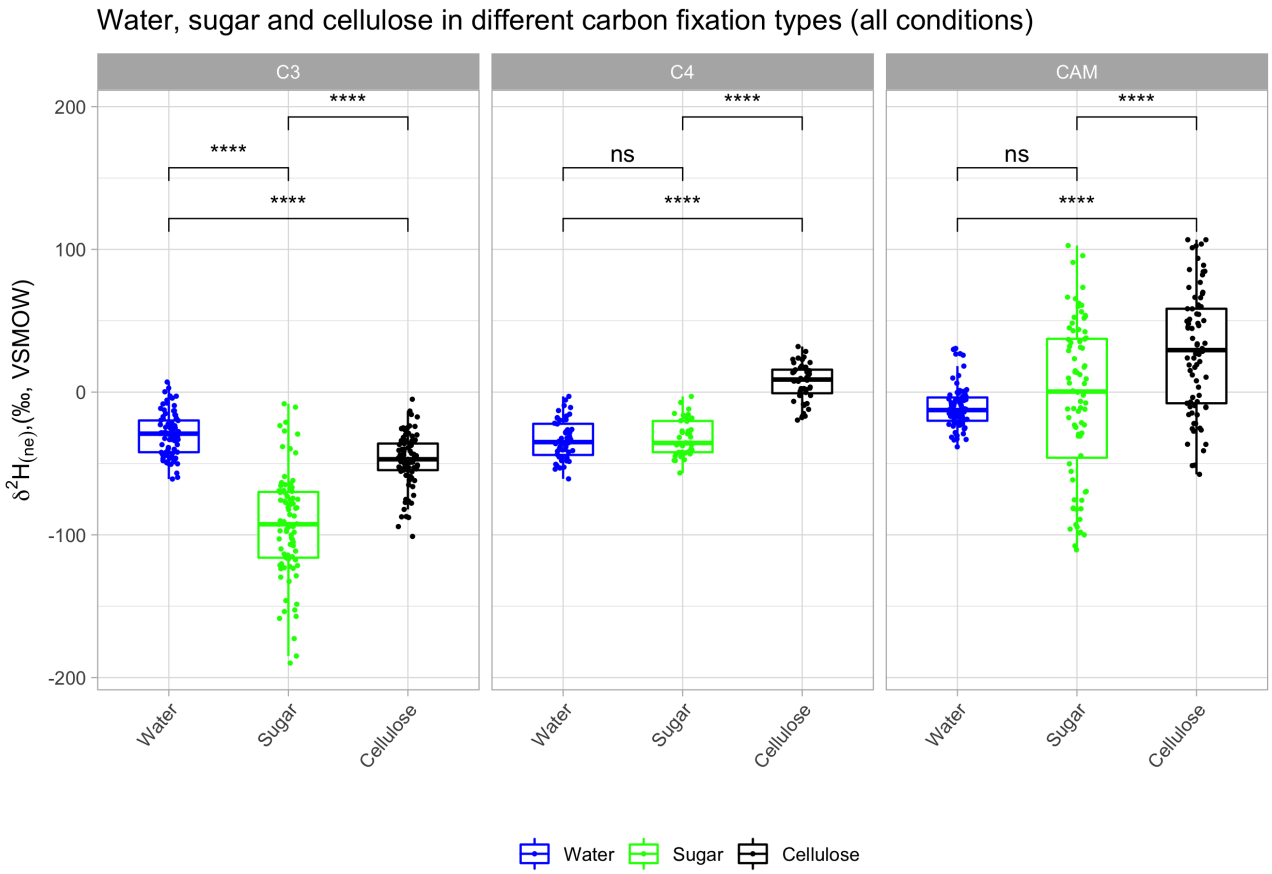

Figure 7: Comparison of $\delta^2H_{(ne)}$ between all compounds (water, sugar, cellulose) and carbon fixation pathways. Data set includes data points from all conditions with results of unpaired t.test. A segregated analysis of each condition on itself was performed and followed the same pattern (not shown). Additional, Tukey multiple comparison of means showed a highly significant difference between all compounds in between carbon fixation types (** to ****) except for δ^2H_{Water} of C_3-C_4 plants (n.s.).

Table 3: Mean $\delta^2H_{(ne)}$ values in ‰ of the different compounds displayed in Figure 7.

	C_3		**C_4**		**CAM**	
	Mean [‰]	SD	Mean [‰]	SD	Mean [‰]	SD
δ^2H water	-29.5	14.8	-33.3	13.8	-10.3	15.6
δ^2H_{ne} sugar	-93.1	36.7	-32.0	12.6	5.3	55.4
δ^2H_{ne} Cellulose	-47.7	18.1	7.3	13.8	29.1	42.5

4.2 Linear models comparing plant compounds

Linear models were done for all combinations of the plant compounds and are shown in Figures 8 to 10. The numerical results including R^2, p-values and the model equations are shown in Table 4.

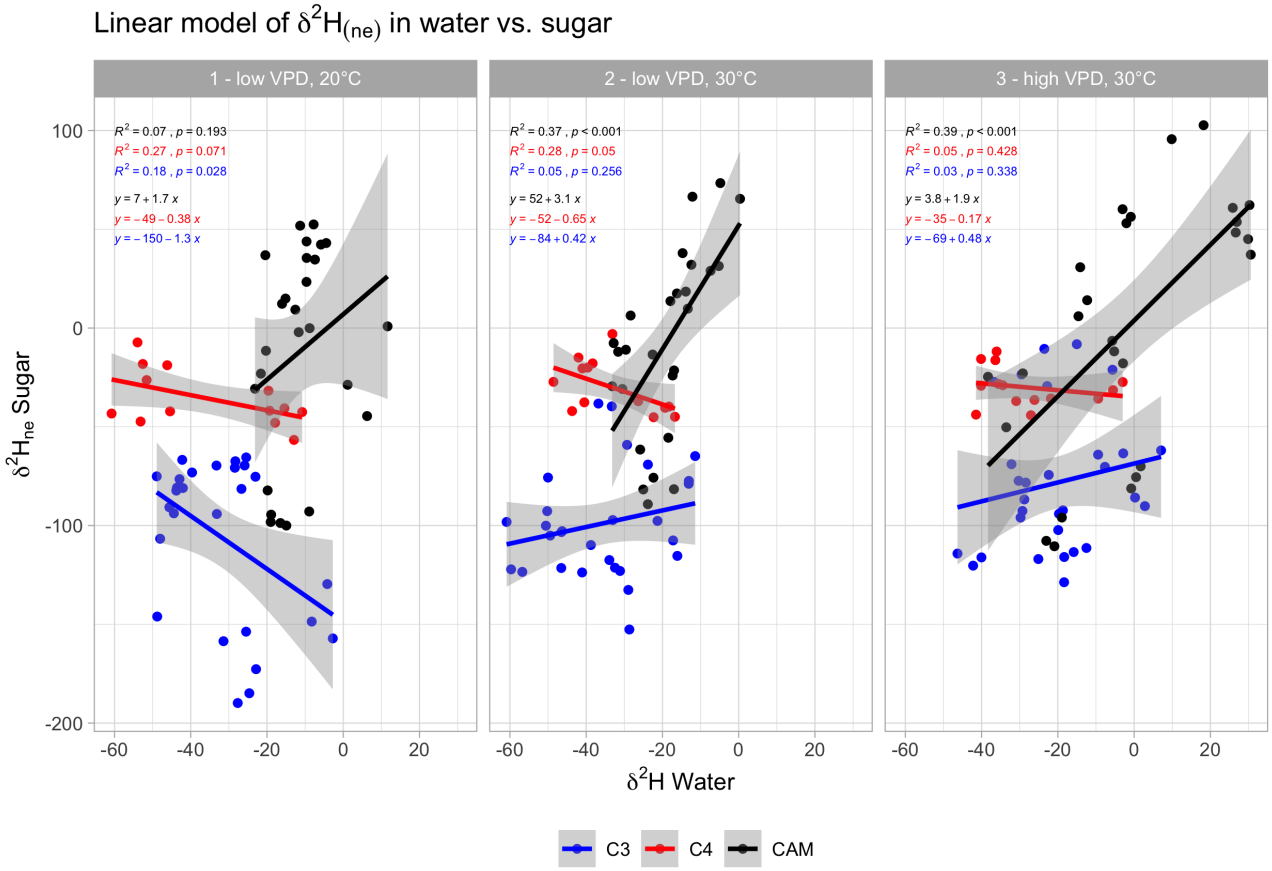

Figure 8: Linear model of $\delta^2H_{(ne)}$ water vs. sugar of each carbon fixation type within specific growing condition.

In Figure 8 the linear model between $\delta^2H_{(ne)}$ water and sugar is shown. In general, C_3 plants have the lowest $^2H_{ne}$ sugar values indicating a strong depletion of ^2H during photosynthesis. Whereas CAM plants have the highest values showing values well over 0‰. The C_4 plants are positioned in the middle of both C_3 and CAM plants.

Starting from first condition (low VPD, 30°C), C_3 species have a strong negative correlation between water and sugar samples. However, the slope becomes positive in the second (low VPD, 30°C) and third condition (high VPD, 30°C). The opposite is visible when looking at CAM species. Here, the slope is clearly positive with the highest inclination in the second condition, with a slope value of 3.1. Interestingly, the CAM species have the largest spread in the third condition, about 70‰ for water and 200‰ for sugar. In contrast, the $\delta^2H_{(ne)}$ values of the C_4 species are relatively consistent between the different conditions with a slightly negative correlation.

Comparing these results from Figure 8 with Figure 9, where δ^2H water vs. δ^2H_{ne} cellulose is shown, they look similar. C_3 plants have a negative correlation in the first condition and then a positive correlation in the second and third condition. For the CAM species the overall trend is the same as in the water-sugar comparison, but here the slopes are much smaller (between 0.55 - 0.93) compared to before (1.7 - 3.1).

One major difference can be found in the data from C_4 plants, where the slope is now positively correlated, whereas before it was slightly negative. Furthermore, the δ^2H_{ne} cellulose values of C_4 and CAM plants are now closer together.

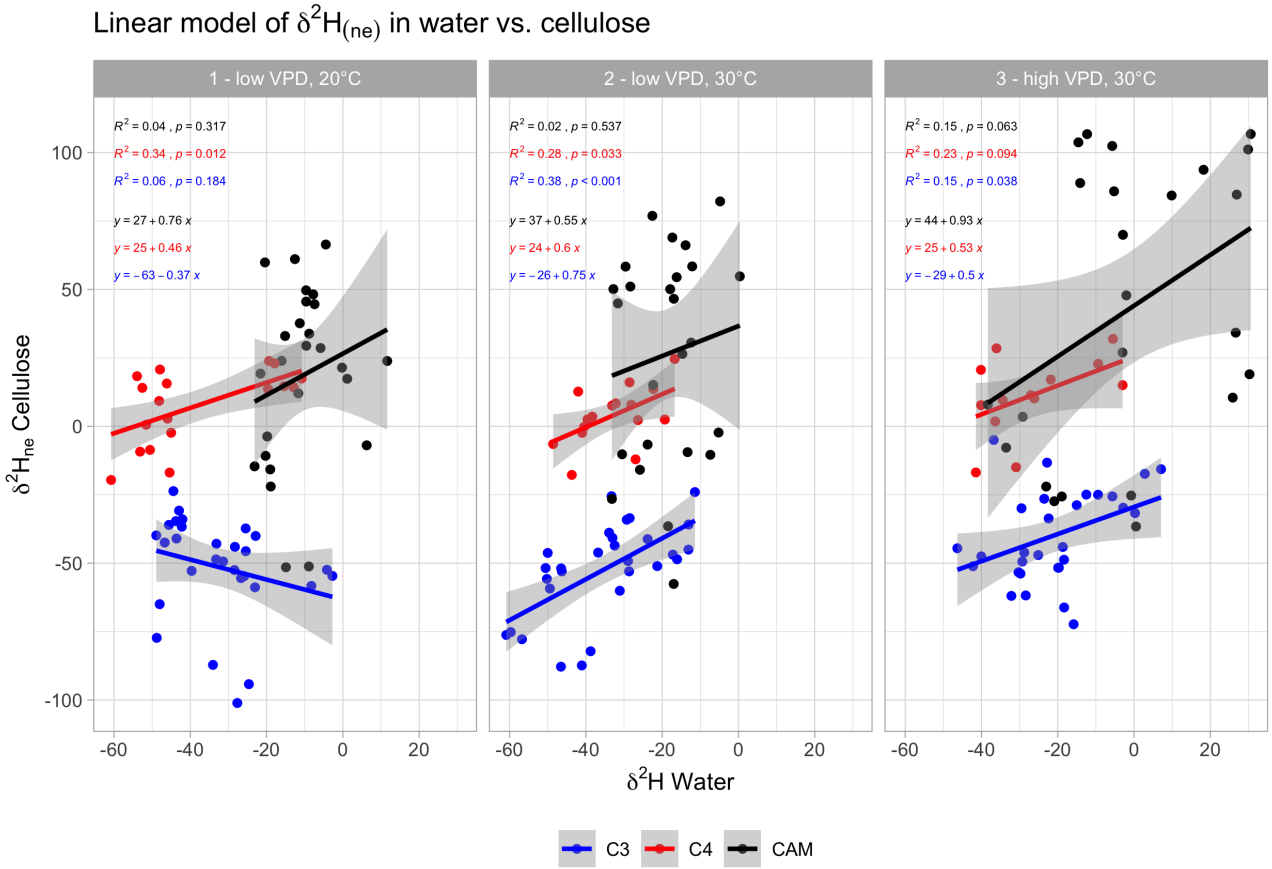

Figure 9: Linear model of $\delta^2H_{(ne)}$ water vs. cellulose of each carbon fixation type within specific growing condition.

When comparing δ^2H_{ne} sugar vs. cellulose in Figure 10, all the correlations are more or less positive and stable between the different conditions. Moreover, the data points of the C_4 species have a much smaller variation in the $^2H_{ne}$ composition compared to the other two carbon fixation pathways. Also the δ^2H_{ne} cellulose values of C_3 plants are more depleted in ^2H compared to C_4, which is situated within the results of CAM species. Overall, the different carbon fixation types have a similar correlation, unlike the correlations from Figures 8 and 9. When the linear model is applied without accounting for the carbon fixation pathway, a significant correlation can be observed, see Figure 11.

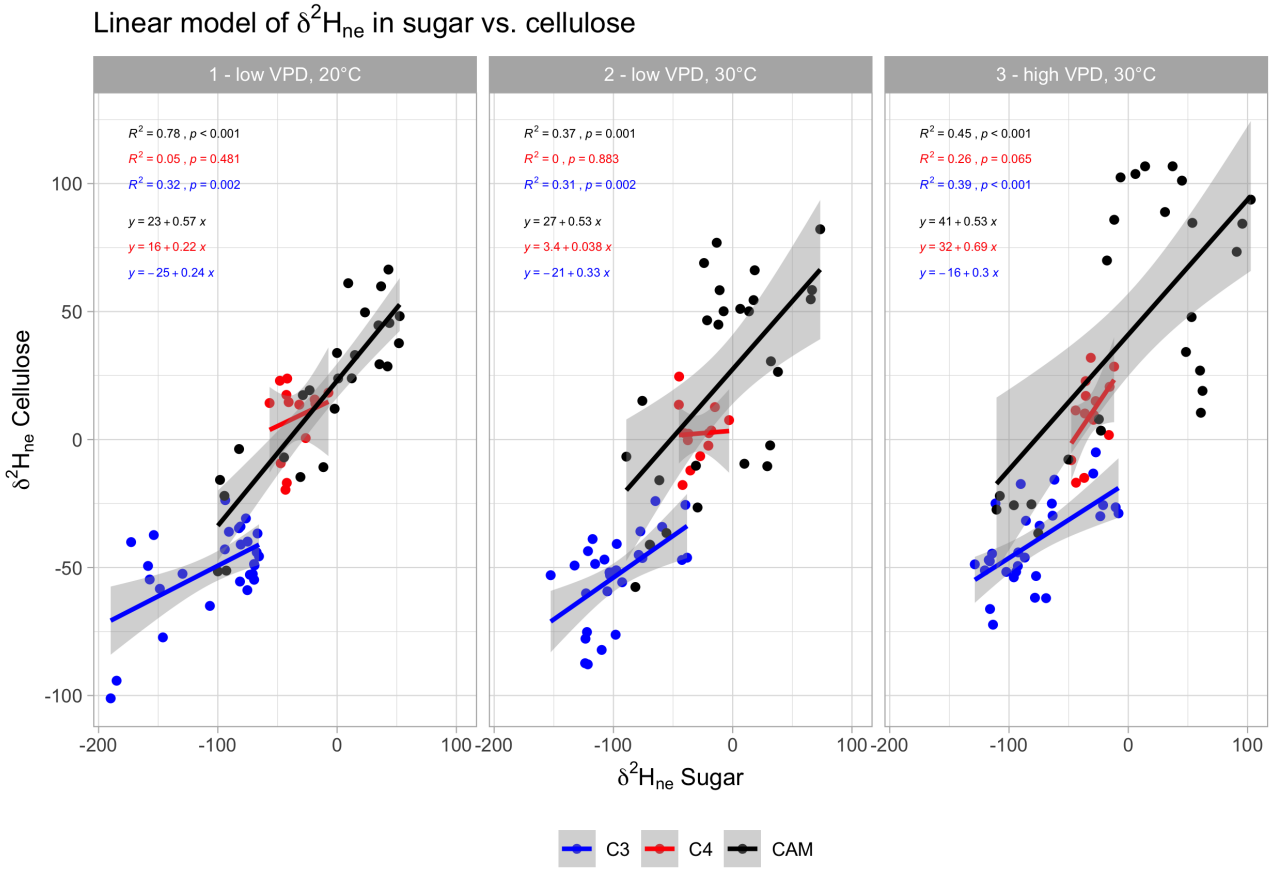

Figure 10: Linear model of $\delta^2H_{(ne)}$ sugar vs. cellulose of each carbon fixation type within specific growing condition.

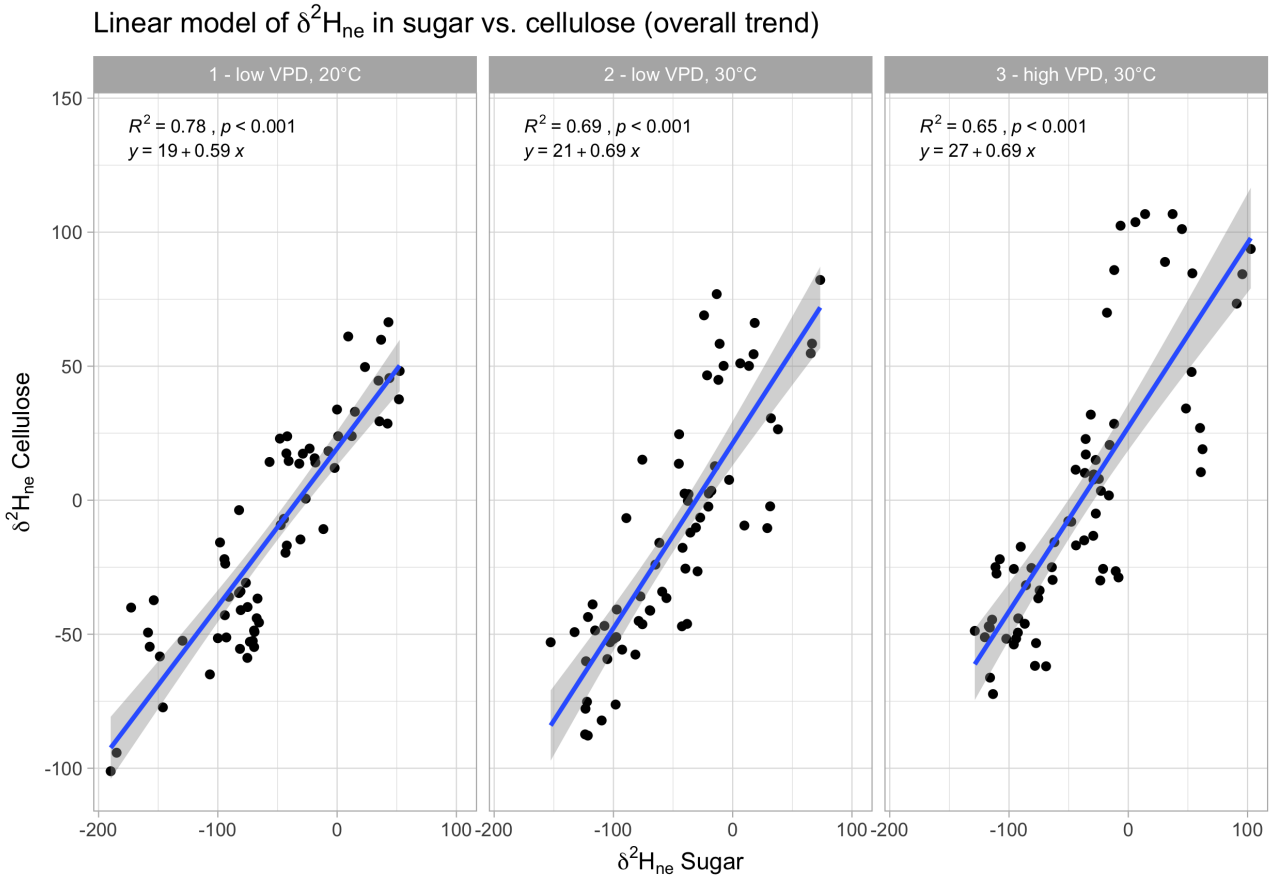

Figure 11: Linear model of $\delta^2H_{(ne)}$ sugar vs. cellulose within specific growing condition not accounting for different carbon fixation types.

Table 4: Correlation table with R^2, p-values and linear model equation including slope.

		corr(water, sugar)				corr(water, cellulose)				corr(sugar, cellulose)			
		R^2	p-value	lm eq.	lm slope	R^2	p-value	lm eq.	lm slope	R^2	p-value	lm eq.	lm slope
low VPD, 20°C	C_3	0.18	0.028	-150 - 1.3 x	-1.30	0.06	0.184	-63 - 0.37 x	-0.37	0.32	0.002	-15 + 0.24 x	0.24
	C_4	0.27	0.071	-49 - 0.38 x	-0.38	0.34	0.012	25 + 0.46 x	2.00	0.05	0.481	16 + 0.22 x	0.22
	CAM	0.07	0.193	7 + 1.7 x	1.70	0.04	0.317	27 + 0.76 x	0.76	0.78	<0.001	23 + 0.57 x	0.57
low VPD, 30°C	C_3	0.05	0.256	-84 + 0.42 x	0.42	0.38	<0.001	-26 + 0.75 x	0.75	0.31	0.002	-21 + 0.33 x	0.33
	C_4	0.28	0.05	-52 + 0.65 x	0.65	0.28	0.033	24 + 0.6 x	0.60	0	0.883	3.4 + 0.038 x	0.04
	CAM	0.37	<0.001	52 + 3.1 x	3.10	0.02	0.537	37 + 0.55 x	0.55	0.37	0.001	27 + 0.53 x	0.53
high VPD, 30°C	C_3	0.03	0.228	-69 + 0.48 x	0.48	0.15	0.038	-29 + 0.5 x	0.50	0.39	<0.001	-16 + 0.3 x	0.30
	C_4	0.05	0.428	-35 - 0.17 x	-0.17	0.23	0.094	25 + 0.53 x	0.53	0.26	0.065	32 + 0.69 x	0.69
	CAM	0.39	<0.001	3.8 + 1.9 x	1.90	0.15	0.063	44 + 0.93 x	0.93	0.45	<0.001	41 + 0.53 x	0.53

4.3 Biological fractionation factors

In Figures 13 and 12 box plots of ϵbioHA and ϵbioHE for all carbon fixation types and climatic condition are shown.

The comparison for the climatic conditions within each carbon fixation type were all not significantly different (Figure 12). This can be explained by the different temperature and VPD optimum conditions, which are species specific. In warmer conditions, some of the species have a e.g. lower ϵbioHA indicating a higher temperature optimum (Schuler et al., 2021). Where as plants with a lower temperature optimum exhibit a smaller ϵbioHA, thus cancelling each other out.

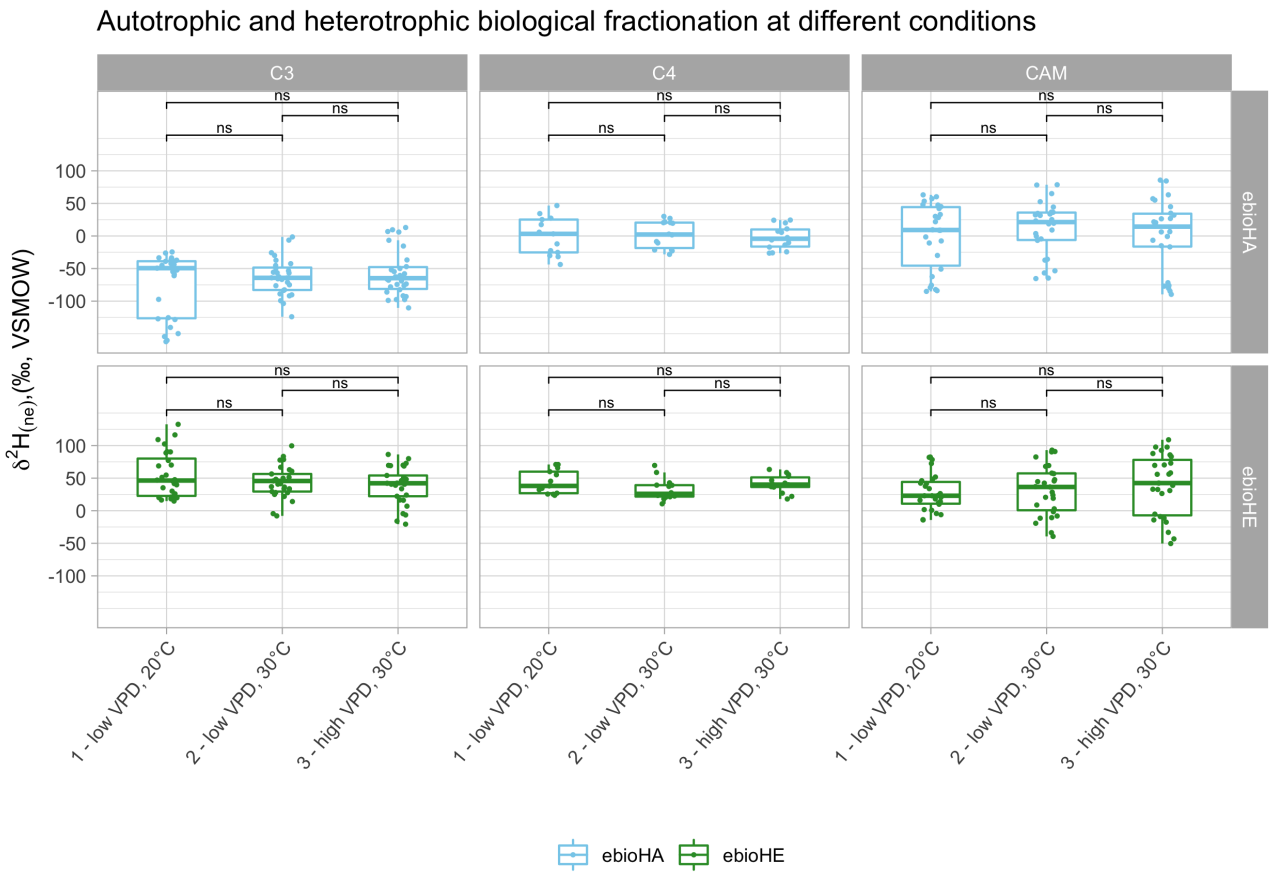

Figure 12: Statistical analysis of ϵbioHA and ϵbioHE comparing the different conditions (unpaired t.test).

However, in between carbon fixation types there are differences (Figure 13). All comparisons of ϵbioHA (δ^2H_{ne} sugar - δ^2H water) show the same general trend. C_3 species are significantly more negative than C_4 and CAM species. However, the ϵbioHA of C_4 and CAM species is not significantly different under each condition. The ϵbioHE (δ^2H_{ne} cellulose - δ^2H_{ne} sugar) are not significantly different within one climatic condition with one exception being C_3 and CAM species at low VPD, 20°C.

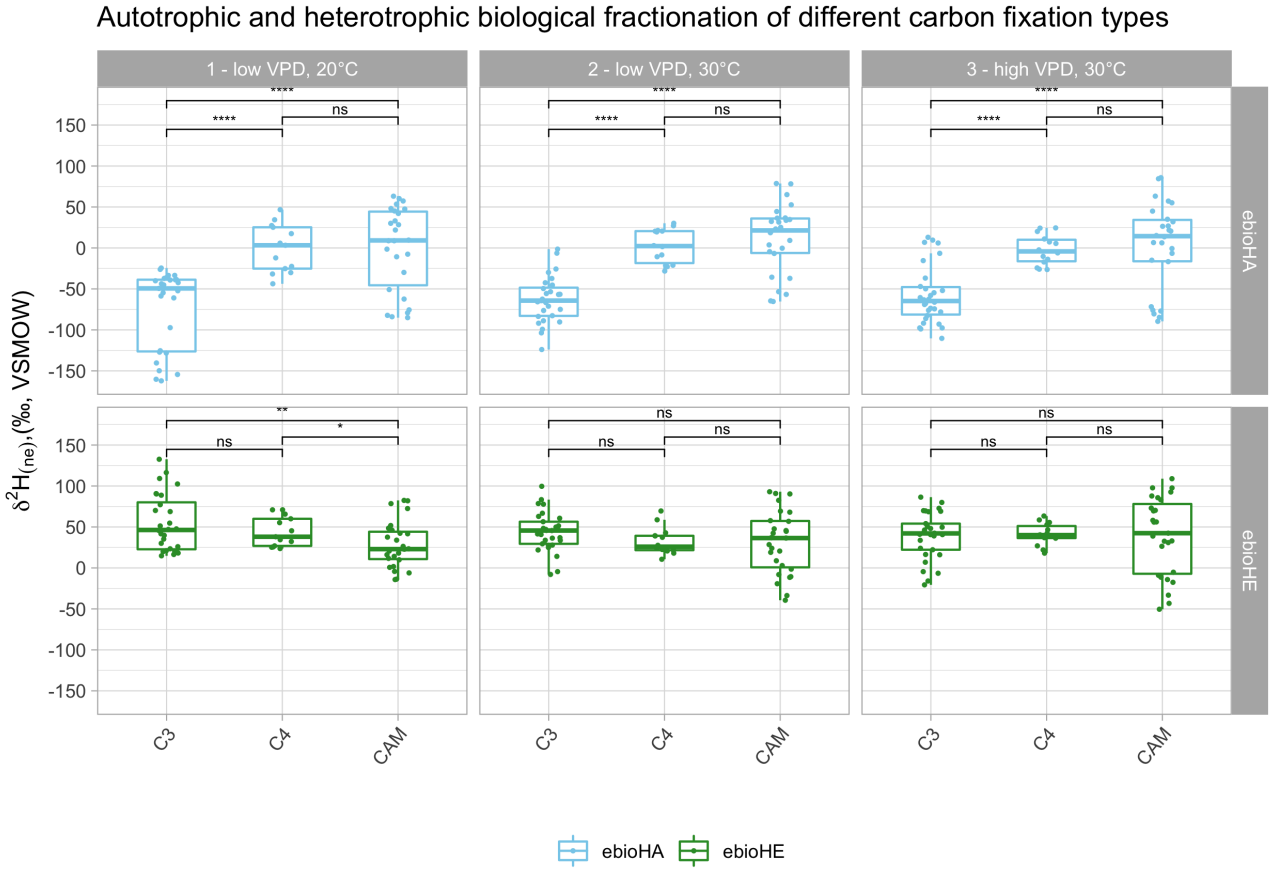

Figure 13: Statistical analysis of ϵbioHA and ϵbioHE comparing the different carbon fixation types (unpaired t.test).

4.4 ANOVAs

Several ANOVAs were performed looking at the relationship of one specific plant compound or biological fractionation factor to the interaction of species and temperature or VPD effect, respectively. The results are shown in Tables 5 to 9. In general the species factor was significant for all compounds and climatic conditions.

Water
The ANOVA results concerning the water samples are shown in Table 5. Here, the species and climatic factors as well as the interactions are highly significant.

Table 5: ANOVA results of Water ∼ Species∗Temperature or VPD. Shows if the influence of temperature or VPD is significant for δ^2H of water for each carbon fixation type.

	Water ∼ Species∗Temperature or VPD							
	Temperature				**VPD**			
		F value	*Pr(<F)*			*F value*	*Pr(<F)*	
C_3	*Species*	56.04	2.00E-16	***	*Species*	11.85	5.51E-11	***
	Temp.	10.43	0.00256	**	*VPD*	46.356	3.13E-09	***
	Sp.:Temp.	33.8	1.87E-15	***	*Sp.:VPD*	3.788	0.00065	***
C_4	*Species*	88.71	2.96E-14	***	*Species*	32.875	3.68E-13	***
	Temp.	25.93	3.71E-05	***	*VPD*	12.924	0.00088	***
	Sp.:Temp.	11.7	1.04E-05	***	*Sp.:VPD*	7.925	2.91E-05	***
CAM	*Species*	11.491	8.06E-08	***	*Species*	24.74	< 2.00E-16	***
	Temp.	34.729	1.07E-06	***	*VPD*	79.26	1.25E-12	***
	Sp.:Temp.	4.325	0.00107	**	*Sp.:VPD*	11.06	1.70E-09	***

Sugar
When looking at the sugar samples, the ANOVA results stay the same as in the water data set for the C_3 species. In C_4 species, the climatic condition and the species-climatic condition interactions are not significant. Mixed results are observed in CAM species, there was no significance for temperature alone but for the species and the species:temperature interaction. However, the VPD and the species interaction was highly significant.

Table 6: ANOVA results of Sugar ∼ Species∗Temperature or VPD. Shows if the influence of temperature or VPD is significant for δ^2H_{ne} of sugar for each carbon fixation type.

	Sugar ∼ Species∗Temperature or VPD							
	Temperature				**VPD**			
		F value	*Pr(<F)*			*F value*	*Pr(<F)*	
C_3	*Species*	45.11	< 2e-16	***	*Species*	15.774	1.80E-13	***
	Temp.	10.8	0.00222	**	*VPD*	25.187	4.08E-06	***
	Sp.:Temp.	20.63	7.29E-12	***	*Sp.:VPD*	5.942	4.52E-06	***
C_4	*Species*	7.874	0.00075	***	*Species*	6.484	0.00027	***
	Temp.	3.479	0.07853	.	*VPD*	0.033	0.85721	
	Sp.:Temp.	1.163	0.35992		*Sp.:VPD*	0.704	0.55634	
CAM	*Species*	174.218	< 2e-16	***	*Species*	160.96	< 2e-16	***
	Temp.	1.054	0.312		*VPD*	27.67	1.89E-06	***
	Sp.:Temp.	8.947	1.39E-06	***	*Sp.:VPD*	4.23	0.00043	***

Cellulose
Here the temperature effect was only barely significant for CAM species (also with the interaction). For C_3 species, the species:temperature interaction was significant, whereas in C_4 species they are both non significant. For the VPD effect, both C_3 and CAM plants showed significant results. And similarly to the temperature effect, C_4 was an exception and not significant.

Table 7: ANOVA results of Cellulose ∼ Species∗Temperature or VPD. Shows if the influence of temperature or VPD is significant for δ^2H_{ne} of cellulose for each carbon fixation type.

	Cellulose ∼ Species∗Temperature or VPD							
	Temperature				**VPD**			
		F value	*Pr(<F)*			*F value*	*Pr(<F)*	
C_3	*Species*	14.696	3.86E-10	***	*Species*	3.386	0.00172	**
	Temp.	0.297	0.589		*VPD*	14.121	0.00036	***
	Sp.:Temp.	25.286	8.08E-14	***	*Sp.:VPD*	4.032	0.00035	***
C_4	*Species*	3.524	0.0172	*	*Species*	5.511	0.00069	***
	Temp.	0.933	0.3445		*VPD*	3.078	0.08764	.
	Sp.:Temp.	0.745	0.598		*Sp.:VPD*	1.262	0.30238	
CAM	*Species*	44.723	7.92E-16	***	*Species*	44.537	< 2e-16	***
	Temp.	4.297	0.0458	*	*VPD*	31.077	6.49E-07	***
	Sp.:Temp.	8.077	4.81E-06	***	*Sp.:VPD*	4.637	0.0002	***

Autotrophic biological fractionation
The temperature and VPD are significant for C_3 species, with lower p-values for the VPD alone. The ϵbioHA showed significant results for VPD and interaction and no significance for the temperature effect. In CAM plants, the opposite was the case, with significance of temperature but none for the VPD effect.

Table 8: ANOVA results of ϵbioHA ∼ Species∗Temperature or VPD. Shows if the influence of temperature or VPD is significant for ϵbioHA for each carbon fixation type.

	ϵbioHA ∼ Species∗Temperature or VPD							
	Temperature				**VPD**			
		F value	*Pr(<F)*			*F value*	*Pr(<F)*	
C_3	*Species*	46.31	< 2e-16	***	*Species*	19.984	1.43E-15	***
	Temp.	14.94	0.00046	***	*VPD*	4.091	0.0472	*
	Sp.:Temp.	13.75	4.16E-09	***	*Sp.:VPD*	5.955	4.88E-06	***
C_4	*Species*	53.393	2.10E-09	***	*Species*	43.212	4.55E-13	***
	Temp.	0.625	0.44		*VPD*	9.22	0.00482	**
	Sp.:Temp.	1.569	0.228		*Sp.:VPD*	2.923	0.0494	*
CAM	*Species*	127.452	< 2e-16	***	*Species*	106.906	<2e-16	***
	Temp.	12.79	0.00107	**	*VPD*	0.224	0.638	
	Sp.:Temp.	7.226	1.46E-05	***	*Sp.:VPD*	1.675	0.123	

Heterotrophic biological fractionation
The ϵbioHE results were similar to ϵbioHA. Moreover, C_3 plants showed a higher significance with VPD. There was only a small significance with the temperature in C_4 species and no interaction can be observed. At last, in CAM plants only the temperature interaction was significant, but not the temperature alone. Although, VPD and VPD interaction were significant as well.

Table 9: ANOVA results of ϵbioHE $\sim$ Species$*$Temperature or VPD. Shows if the influence of temperature or VPD is significant for ϵbioHE for each carbon fixation type.

	ϵbioHE $\sim$ Species$*$Temperature or VPD							
	Temperature				**VPD**			
		F value	*Pr(<F)*			*F value*	*Pr(<F)*	
C_3	*Species*	40.444	< 2e-16	***	*Species*	29.515	< 2e-16	***
	Temp.	16.744	0.00022	***	*VPD*	11.572	0.00114	**
	Sp.:Temp.	4.989	0.0002	***	*Sp.:VPD*	7.729	1.16E-07	***
C_4	*Species*	15.272	1.80E-05	***	*Species*	9.933	9.62E-06	***
	Temp.	5.734	0.0284	*	*VPD*	5.012	0.0325	*
	Sp.:Temp.	0.931	0.4693		*Sp.:VPD*	1.617	0.2056	
CAM	*Species*	20.786	2.45E-11	***	*Species*	27.853	<2e-16	***
	Temp.	0.425	0.51873		*VPD*	4.1	0.0471	*
	Sp.:Temp.	4.871	0.0004	***	*Sp.:VPD*	2.538	0.0184	*

4.5 Temperature optimum of all species

The species specific temperature dependent data (ϵbioHA) was plotted for all carbon fixation types, to acquire a visual overview of the optimal growing temperature (Figures 14 to 16). The results of the unpaired t.test comparison between the ϵbioHA values of high and low temperature conditions are shown in Table 10.

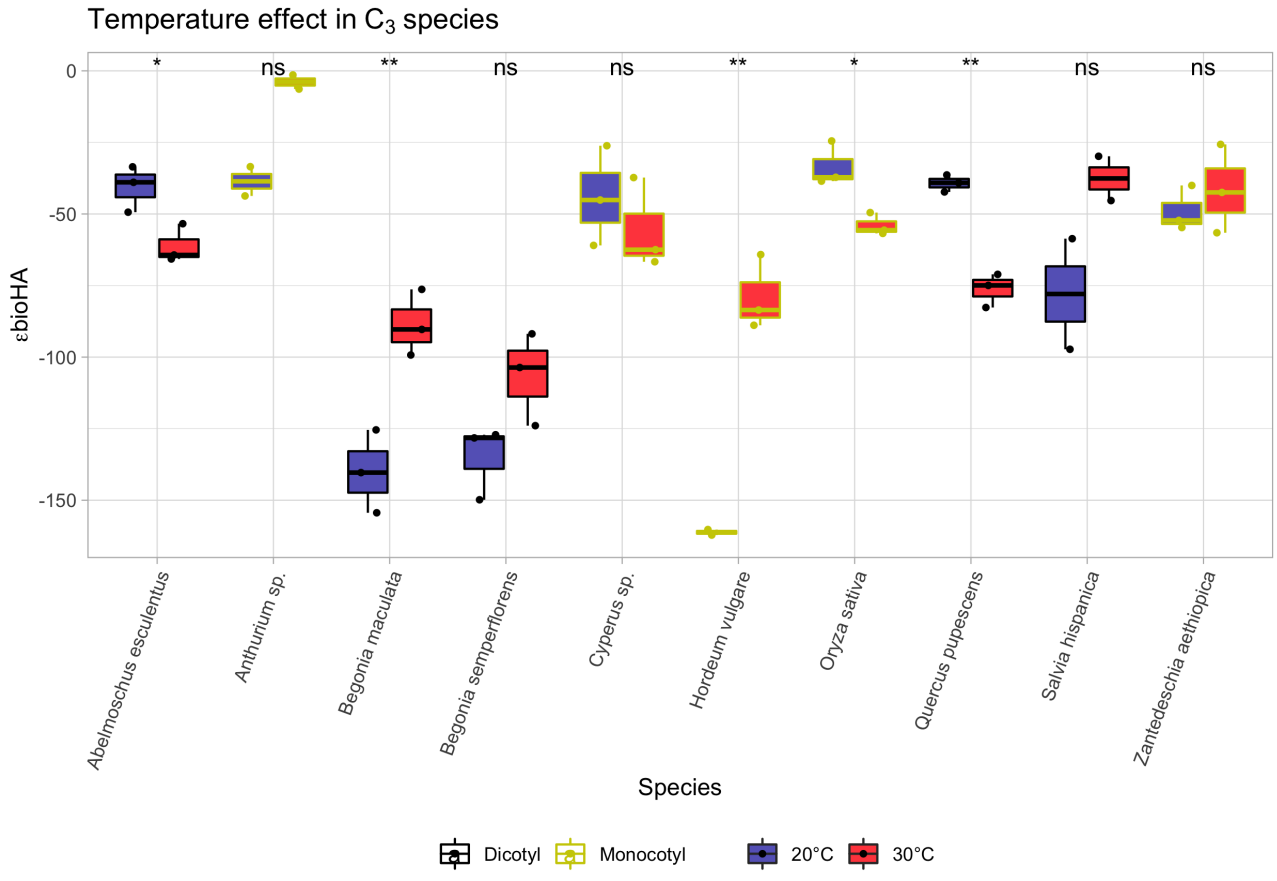

Figure 14: Shows the temperature difference of ϵbioHA in C_3 plants and if the belong to the mono- or dicots. Data set is a subset with data points with the same VPD conditions (low). The level of significance from unpaired t.test is indicated on top.

C_3

In Figure 14 showing the ϵbioHA values all C_3 species, the species can be put in two groups. Most of the species have ϵbioHA values around -50‰. Both *Begonia* species and *Hordeum vulgare* have ϵbioHA values between -100 to -150‰, thus having a much larger difference between δ^2H_{ne} sugar and δ^2H water. Additionally, both groups are a mix of mono- and dicots. But not clear trend was visible. Furthermore, *Anthurium sp.* has only two data points for each condition. The differences between 20°C and 30°C for each species are not always significant. Furthermore, they can not be assigned to one group or the other, however, the group with the larger ϵbioHA values, has more positive ϵbioHA values at 30°C.

C_4

The C_4 plants are represented with 4 species, as a result of insufficient data points for the statistical analysis. Here, two groups can be made with mono- and dicots. Dicotyl species have clearly negative ϵbioHA values, whereas the monocotyl species have all positive ϵbioHA values. Here the differences between temperature conditions is not as clear as in Figure 14 with the C_3 species. Thus, the unpaired t.test was not significant for all cases.

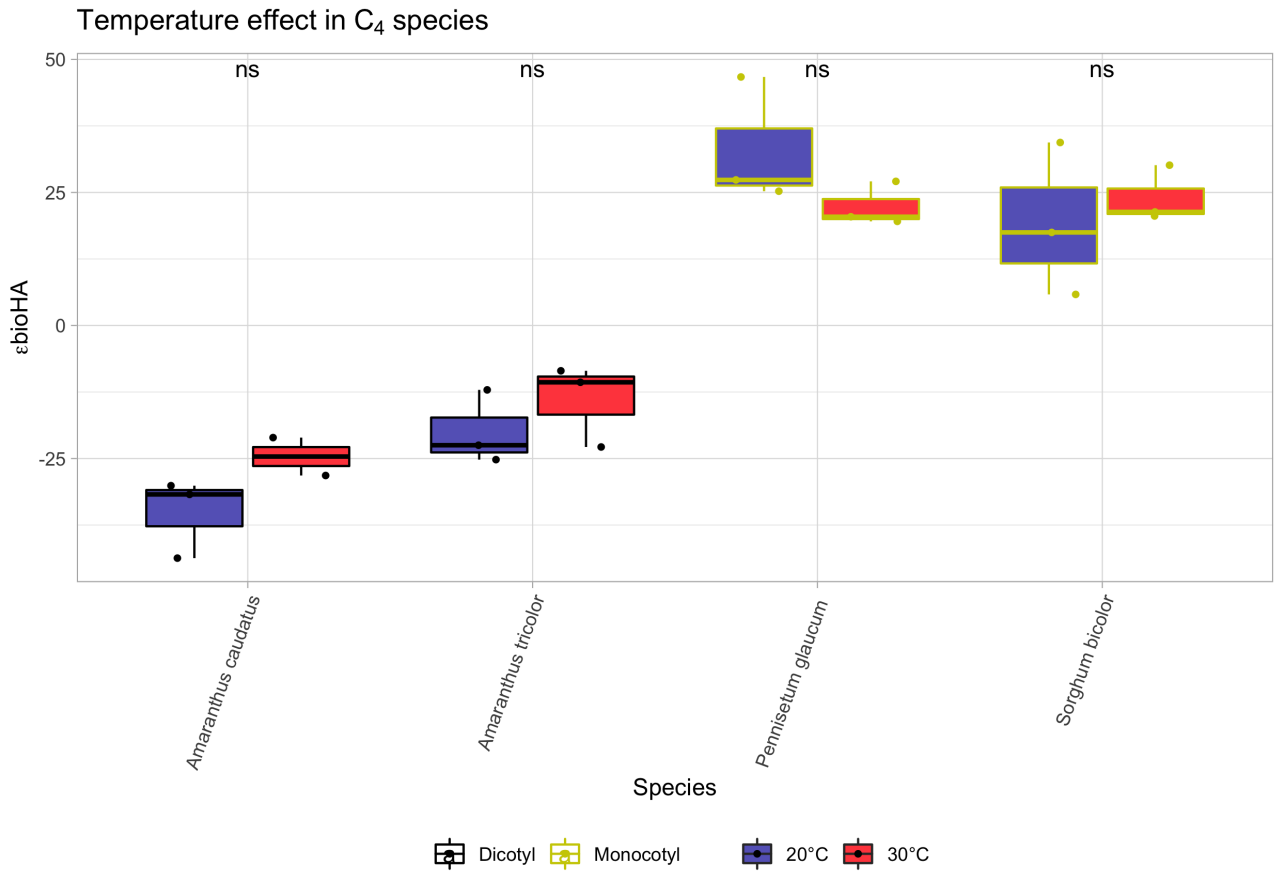

Figure 15: Shows the temperature difference of ϵbioHA in C_4 plants and if the belong to the mono- or dicots. Data set is a subset with data points with the same VPD conditions (low). The level of significance from unpaired t.test is indicated on top. Results from *Setaria italica* and *Zea mays* are missing, because there were not enough data points for the statistical analysis.

CAM

The CAM plants do not have the similar clear differentiation as C_3 and C_4 species. Four species have clearly positive ϵbioHA values (*Hylocereus sp., Phalaenopsis, Rhipsalis sp.* and *Salsola soda*). On the opposite site of the spectrum are *Aptenia cordifolia* and *Delosperma sp.* with ϵbioHA values around -60‰. The rest of the species have ϵbioHA values around 0‰, in other words no biological fractionation. Moreover, the temperature effect was significant in only three species.

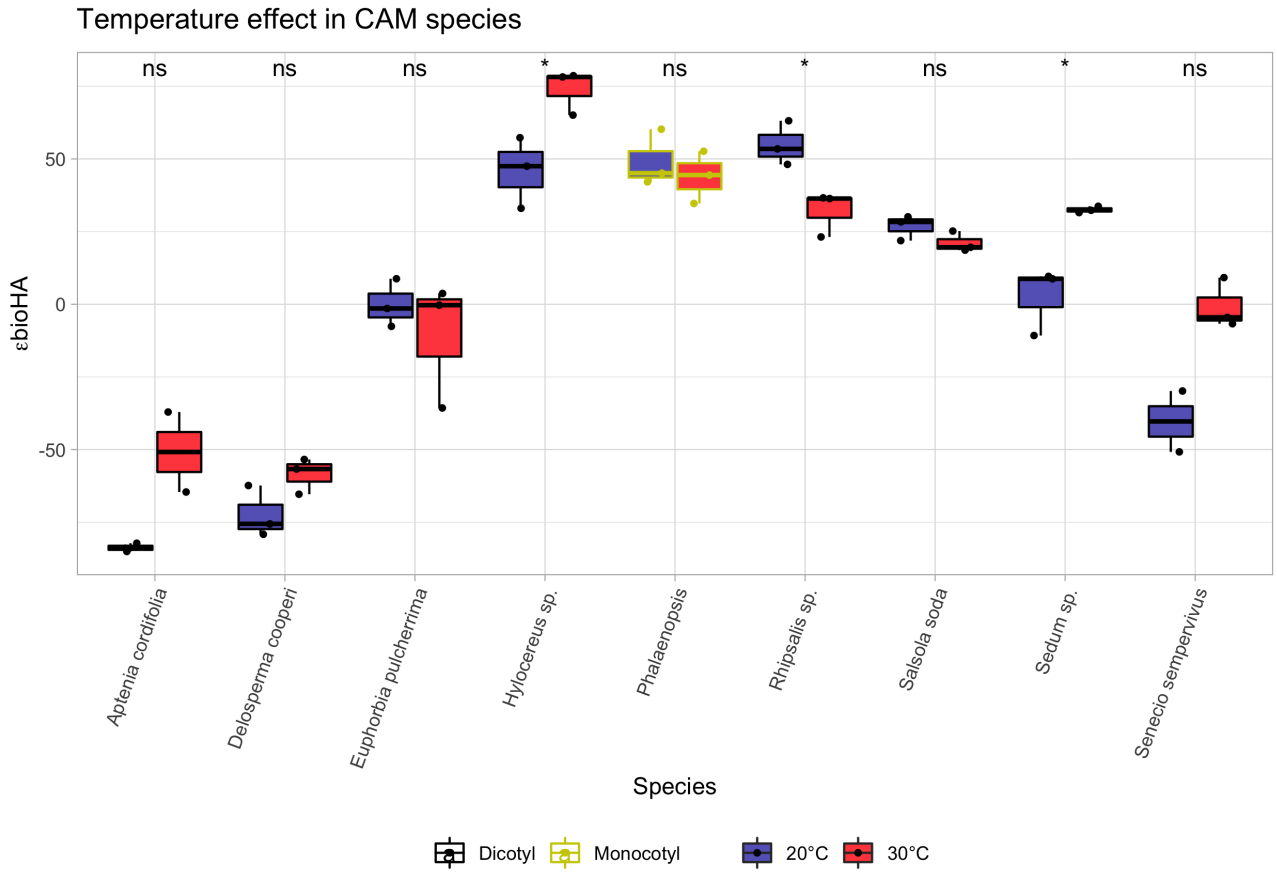

Figure 16: Shows the temperature difference of ϵbioHA in CAM plants and if the belong to the mono- or dicots. Data set is a subset with data points with the same VPD conditions (low). The level of significance from unpaired t.test is indicated on top.

Table 10: Temperature optimum of all species, based on ϵbioHA. The level of significance from unpaired t.test is indicated on top. The temperature optima were determined visually from Figures 14 to 16, by which temperature showed the lower ϵbioHA values. If there was no clear lower ϵbioHA values in a species, "+/-" was used. Results from *Setaria italica* and *Zea mays* are missing, because there were not enough data points for the statistical analysis.

	Species	**Temperature optimum [°C]**	**Signif.**
C3	*Abelmoschus esculentus*	30	*
	Anthurium sp.	20	ns
	Begonia maculata	20	**
	Begonia semperflorens	20	ns
	Cyperus sp.	30	ns
	Hordeum vulgare	20	**
	Oryza sativa	30	*
	Quercus pupescens	30	**
	Salvia hispanica	20	ns
	Zantedeschia aethiopica	+/-	ns
C4	*Amaranthus caudatus*	20	ns
	Amaranthus tricolor	+/-	ns
	Pennisetum glaucum	30	ns
	Setaria italica	-	-
	Sorghum bicolor	+/-	ns
	Zea mays	-	-
CAM	*Aptenia cordifolia*	20	ns
	Delosperma cooperi	20	ns
	Euphorbia pulcherrima	+/-	ns
	Hylocereus sp.	20	*
	Phalaenopsis	+/-	ns
	Rhipsalis sp.	30	*
	Salsola soda	+/-	ns
	Sedum sp.	20	*
	Senecio sempervivus	20	ns

Chapter 5

Discussion

5.1 Difference in carbon fixation pathways

5.1.1 Carbon fixation type comparison

The analysis of the bulk data set including all climatic conditions shown in Figure 7 showed distinct differences in ^2H composition not only in between compounds but also between carbon fixation pathways. Even though, sugar and cellulose δ^2H_{ne} values generally increased from C_3 to C_4 to CAM plants, C_3 and CAM sugars showed a large variation ranging up to 200‰ for both carbon fixation types. Additionally, also the cellulose values showed high variation in C_3 and CAM plants. At least for CAM plants this larger variation could be explained by the fact, that some CAM species are only facultative CAM species. Thus, the part of the signal could be influence by C_3 and C_4 carbon fixation (Schuler et al., 2021). In general, I obtained similar mean $\delta^2H_{(ne)}$ values as Schuler et al., 2021. But, Sternberg et al., 1984 reported more ^2H depleted cellulose composition for C_4, whereas my results were more enriched.

C_3 plants showed a strong depletion of ^2H in plant sugars compared to leaf water, whereas the δ^2H_{ne} of cellulose was in between the water and sugar values. This depletion in sugar is likely due to ^2H depletion during NADPH formation and later incorporation into NSC (Cormier et al., 2018; Schuler et al., 2021). Ferroxin-$NADP^+$ reductase produces NADPH, with strongly ^2H depleted hydrogen during the light reaction(Luo et al., 1991). NAPDH is later introduced into NSC by the formation of glyceraldehyde-3-phosphate (GAP) (Cormier et al., 2018; Schuler et al., 2021). However, during GAP formation, some of the hydrogen atoms can exchange with the surrounding ("^2H enriched") leaf water, which leads to an enrichment in the GAP pool and therefore post-photosynthetic ^2H enrichment (Cormier et al., 2018). Additionally, only one of the hydrogen atoms in GAP is derived from the depleted NADPH and the rest comes from the GAP precursor 3-PGA, which is enriched due to the leaf water. Thus, leading to less negative cellulose values compared to sugar. Furthermore, if photosynthetic carbohydrate supply is low, the δ^2H_{ne} cellulose values are less negative (Cormier et al., 2018).

C_4 plants on the other hand showed no significant difference between δ^2H water and δ^2H_{ne} sugar. However, the leaf cellulose was enriched in ^2H, compared to water and NSC. Moreover, leaf water of C_3 and C_4 plants were not significantly different. The higher ^2H composition of NSC compared to water is due to the different origin of NADPH (Schmidt et al., 2003). In C_4 plants, NADPH can also come from malate from the mesophyllic cells. This additional NADPH pool leads to a mixture in the signal and thus more enriched NSC compared to C_3 plants. The enrichment of cellulose compared to the leaf water could be due to post-photosynthetic isotope exchange or evaporative effects (Cormier et al., 2018; Sternberg et al., 1984).

The CAM species ^{2}H composition was enriched from water to NSC to cellulose and overall, all compounds are enriched compared to the other two carbon fixation types. However, the variation in NSC and cellulose are large (±100 ‰). Thus, water and sugar ^{2}H composition was not significantly different. The enrichment of leaf water compared to the other two carbon fixation types is in line with the observations of Sternberg et al., 1984. The enrichment effect observed here could, however, also be produced due to the fact, that CAM plants were watered more conservatively. This was done, to ensure that facultative CAM plants are more likely to use CAM as the major carbon fixation pathway. In this case, the loss of water from the tissue through evapotranspiration would lead to an over all enrichment within the leaf (Sternberg et al., 1984, 1986). If this was the case, the oxygen isotope composition would show similar results. However, oxygen isotopes were not analysed for the purpose of this thesis. Moreover, the enrichment of sugar and cellulose tissue can be explained by the additional input of malate as a proton donor during the daytime reaction, similarly as in C_4 plants (Schuler et al., 2021).

Overall, ^{2}H composition of the different plant compounds are statistically different. But, they alone are likely not a good indicator to distinguish between carbon fixation types, because of the overlaps (Sternberg et al., 1984). However, they could be used as an indicator for plant performance (Lehmann, Vitali, et al., 2020).

5.2 Influence of climatic conditions

5.2.1 Linear models

The linear model approach provides the opportunity to see if there are similarities between the fractionation factors in between different carbon fixation types.

When comparing $\delta^2H_{(ne)}$ of water with sugar, it seems that the sugar of C_4 is not dependent on the δ^2H of water. On the other hand, C_3 and CAM plants exhibit a clear trend. C_3 species with high evaporation rates (leaf water more enriched in ^{2}H) have have more depleted sugars. For species with low evaporation, the depletion in the fractionation from water to sugars is smaller. However, this is only the case for the first climatic conditions. In warmer and drier conditions the relationship in C_3 plants changes to a positive correlation, just like in the CAM plants. Here, more enriched water leads to more positive δ^2H_{ne} sugar values. In general, C_3 species exhibit more ^{2}H depleted sugar compared to the other two carbon fixation types. An additional trend of ^{2}H enrichment is the VPD and temperature increase, thus making it harder to distinguish the different carbon fixation types further. This is more visible in C_3 species as the drought and temperature stress is leading to larger evaporation and thus ^{2}H enrichment in leaf water.

In Figure 9 the relationships between water and cellulose look similar to those from Figure 8 (water vs. sugar), although the $\delta^2H_{(ne)}$ cellulose values are overall higher. Furthermore, the C_4 species exhibit a clearer positive correlation and are closer to the CAM species. This would indicate for a similar process of how the water signal is transferred to cellulose for C_4 and CAM species. Interestingly, for C_3 species the same negative correlation as in Figure 8 in the first climatic conditions can be see. Strengthening the assumption that the signal of the sugar is transferred to the cellulose.

This is further reinforced by the results shown in Figure 10 and 11. Here the linear regression lines are so similar, that a linear model for all carbon fixation types combined leads to highly significant results. The increase of temperature and VPD leads to a ^2H enrichment in both leaf sugar and cellulose with a relatively stable constant fractionation relationship (δ^2H_{ne} cellulose = 23 + 0.66 * δ^2H_{ne} sugar, $R^2 = 0.7$, $p < 0.001$). The ^{2}H enrichment in cellulose could be

a results of the usage of different carbohydrate pools (Lehmann, Vitali, et al., 2020). New assimilates are on trend more depleted as those from storage, which had more time to undergo e.g. isotope exchange. During drought stress is is likely, that the availability of new assimilates is low and more storage material is used, therefore leading to an enrichment in the ^{2} composition of cellulose. Additionally, C_4 species seem to have a smaller range of both sugar and cellulose ^{2} composition (about ±50‰). The ranges of C_3 and CAM plants are much larger. Which is for the CAM species, likely a cause of the facultative CAM pathway, as described above.

5.2.2 Biological fractionation factors

Another approach to compare differences in ^{2}H composition can be made with biological fractionation factors. The autotrophic biological fractionation between water and sugar (ϵbioHA) could be used as an indicator of plant performance, with more negative values indicating higher productivity (Schuler et al., 2021). First, ϵbioHA and ϵbioHE were plotted comparing the different climatic conditions within each carbon fixation type, see Figure 12. However, the unpaired t.test showed no significant differences between conditions. This was likely because the species interaction was not taken into account here and the only the climatic conditions were compared. The biological fractionation factors are expected to be constant, but species specific (Schuler et al., 2021).

Nonetheless, when comparing the carbon fixation types in each condition separately a clear pattern can be observed. C_3 plants have a much more negative ϵbioHA, which was significantly different compared to C_4 and CAM plants, in all climatic conditions. While ϵbioHA of C_4 CAM plants can not be separated, CAM plants showed a larger variation in ϵbioHA ranging from +100‰ to -100‰. Interestingly, ϵbioHE did not follow the same pattern. Here, the unpaired t.test comparison was not significant in two conditions, with low significance in the first condition (low VPD, 20°C) but only between CAM vs. C_3 or C_4 plants. This is in line with the observations from the linear models before, where a universal biological fractionation factor between sugar and cellulose was shown.

5.2.3 ANOVA

Several ANOVAs were performed to achieve a better understanding of the effect of temperature and VPD on each plant compound, while accounting for species specific effects.

The ^{2}H composition of water is clearly affected by both temperature and VPD with high significance for all carbon fixation pathways. This was what I expected for C_3 and C_4 species but not for CAM plants. Because, CAM species are adapted for hotter and drier conditions and the carbon fixation is disconnected, see Figure 3. As mentioned before, this could be due to the partial C_3 or C_4 influence in facultative CAM species (Winter, 2019).

The sugar analysis showed similar results for C_3 species with an effect of both climatic factors. This overlaps with the assumption, that in these species the ϵbioHA is highly reactive to climatic changes, thus representing the adaption of photosynthetic processes (Yamori et al., 2013). Hotter and drier environments lead to stomata closure and reduced photosynthetic activity (Yamori et al., 2013). Furthermore, the NADPH generation rate is likely decreased, thus the strong fractionation during the NADHP formation could be smaller, leading to less depleted ^{2}H composition in C_3 sugars (Leaney et al., 1985; Yamori et al., 2013). CAM species showed no effect to temperature, but were highly significant for change in VPD. This might be explained by the disconnect of the carbon fixation. During the day, when the temperature is increased, the stomata are closed and thus the temperature has no effect on the ^{2}H composition during the sugar synthesis. However, the stomata have to open at night to let CO_2 inside the leaf. During this process the plant losses moisture, which in dry conditions can not be compensated

(Sternberg et al., 1986). Moreover, even though if CAM plants showed no significant temperature effect in general, the species interaction was significant. Thus indicating that some of the sample species are facultative CAM plants and likely expressed some C_3 carbon fixation, since no temperature effect was observed in C_4 plants (Winter, 2019).

The ^2H composition of cellulose in C_3 and CAM plants was again significantly affected by the VPD, thus indicating that the VPD effect signal is present in all plant compounds. In C_3 species the temperature effect was species specific, whereas in CAM plant it was significant on its own. This might be because C_3 are closing their stomata faster when confronted with higher temperatures and thus the cellulose synthesis activity is strongly reduced (Sternberg et al., 1986). CAM plants are still producing cellulose in hotter conditions, thus imprinting the enriched signal from the leaf water via post-photosynthetic isotope exchange. Additionally, as before, the facultative CAM plants might be influenced by partially using the C_3 pathway. Differences in C_4 plants were barely significant in the temperature effect subset, suggesting that the cellulose ^2H composition is constant for C_4 species. An argument against this assumption, is the species effect in the VPD effect subset.

The biological fractionation factors (ϵbioHA, ϵbioHE) were proposed to be possible proxy indicators for plant performance (Sanchez-Bragado et al., 2019; Schuler et al., 2021). This was due to the observation of a negative correlation with the stomatal conductance (Sanchez-Bragado et al., 2019). The effects of temperature and VPD were tested in the ANOVAs in Table 8 and 9.

It seems that both fractionation factors could be used to assess the plant performance in C_3 plants, since they where highly significant. In C_4 species a VPD effect is only observable in ϵbioHA, in contrast to the CAM plants, which showed only a temperature effect.

For ϵbioHE, C_4 species where equally significant, but not as strong as for C_3 species. C_3 plants might react stronger to stomatal conductance change and thus photosynthetic activity is reduced via the reduction in CO_2, whereas C_4 plants are able to keep the photosynthetic rate high for longer due to the carbon cummulating mechanism (Sternberg et al., 1984). Furthermore, CAM species were not significant for temperature effects and only barely significant for VPD effects, which is the opposite compared to ϵbioHA.

Summarising, with this experimental set up biological fractionation factors can be used for C_3 species to assess plant performance. The results for C_4 and CAM species might not be as clear for statements concerning the plant performance. The ANOVA results could, however, also be less significant because of the experimental set up. When the species have a wider temperature optimum or the optimum was in between the two tested temperatures (e.g. 25°C), I expect a small difference in ϵbio values.

5.2.4 Temperature optimum

The feasibility of ϵbioHA to estimate the optimum temperature was further analysed in Figures 14 to 16. This species level observation further supports the ANOVA results and trends already seen in Figure 13.

For C_3 plants, most of the differences of ϵbioHA were significantly different and showed strongly negative ϵbioHA values. However, some species showed non significant t.test results. This may most likely to due to the lack of enough data points (*Anthurium sp.*, *Salvia hispanica*). Others might not be significant because the plant performance did not change much in the observed temperatures (*Cyperus sp.*, *Zantedeschia aethiopica*). These species are marsh plants and water was never a limiting factor.

In C_4 plant none of the ϵbioHA between temperatures were significant. The ϵbioHA value were higher compared to C_3 plants indicating a general trend of smaller fractionation between leaf water and sugar. Interestingly, there was a difference between monocotyl and dicotyl species. Monocots seem to have ϵbioHA around 25‰, whereas dicots exhibit the exact opposite with ϵbioHA around -25‰. This trend was also observed by Liu et al., 2016, were leaf wax was more negative in dicotyl species.

Overall the highest (more positive) ϵbioHA values were seen in CAM plants. Some non significan species can again be explained by the lack of data points (*Aptenia cordifolia*, *Senecio sempervivus*). Furthermore, the differences of facultative CAM plants are clearly visible. *Aptenia cord.* and *Delosperma sp.* have ϵbioHA around -50‰, which would indicate C_3 carbon fixation. Furthermore, the dicot species *Euphorbia pulcherrima* shows no temperature effect and is in between CAM and dicot C_4 plants, making it likely that some C_4 carbon fixation was present. The same might be true for *Sedum sp.* and *Salsola soda*, but maybe the influence of C_4 was not as pronounced as in *Sedum sp.*, since the temperature effect was similar compared the other CAM species. Even though, the overall ϵbioHA values were lower. Indeed, these five species are all facultative CAM species (Fleta-Soriano et al., 2015; Webster et al., 1975; Winter, 2019; Winter et al., 2008).

Regardless, of the questionable feasibility to use ϵbioHA as a proxy indicator for plant performance for C_4 and CAM plants, ϵbioHA could also be used to distinguish between different modes of carbon fractionation. This could further help to e.g identify facultative CAM plants. A interesting case hereby is provided by *Salsola soda*. In the the seedling stage *Salsola soda* performes C_3 carbon fixation and then changes to C_4 in adult leaves (Lauterbach et al., 2016). The δ^2H_{ne} sugar are clearly positive indicating CAM metabolism. However, not as positive as obligatory CAM species (e.g. *Hylocereus sp.*) (Wang et al., 2019).

5.3 Limitations

One of the major unknowns is the δ^2H_{ne} cellulose data. As already mentioned above, some of the samples had to be extracted in the tube, as compared to the well established bag method. Several samples of different carbon fixation pathways and species were prepared with both methods, to function as a control. While the results for C_3 and C_4 species were relatively consistent, the CAM species had large differences in certain samples, on average -35.6 $\pm$ 48.6 ‰. Leading to an artificial change in ϵbioHE for example.

Furthermore, three replicates per sample and condition was the bare minimum. With more replicates the effects could be more significant and I would have been able to compare more species. Additionally, some samples had to be left out, as they were lost during preparation.

Chapter 6

Conclusion

In conclusion, with the newly established water-vapour equilibration method I was able to measure different plant compounds including NSC of a variety of species with different modes of carbon fixation. Thus, acquiring a better understanding of the ^{2}H composition change from water to sugar to cellulose.

I was able to observe significant differences in the ^{2}H composition between the different carbon fixation types. C_3 plants showed a strong depletion in sugar compared to the leaf water. This could be due to the input of strongly depleted NADPH. Whereas for C_4 plants the sugar was similar to the ^{2}H composition of of the leaf water, likely cause by the input of malate. Interestingly, the cellulose of C_4 species was then enriched in comparison to the leaf water, which is in line with the observation of a linear relationship between δ^2H_{ne} leaf sugar and cellulose. The CAM species showed similar results as the C_4 plants, however the $\delta^2H_{(ne)}$ was generally higher in CAM plants compared to the other two carbon fixation types. The cellulose had the highest δ^2H_{ne} values in all carbon fixation types.

The biological fractionation factors ϵbioHA and ϵbioHE can be used as a proxy indicator for plant performance. The best results are, however, achieved in C_3 plants. C_4 and CAM plants showed less significant or no significant relationship for temperature and VPD.

Additionally, CAM species were in contrast to my hypothesis, also affected by VPD, but not by temperature. This could be due to the disconnect of the CAM photosynthetic pathway.

In general, leaf water showed an ^{2}H enrichment with higher VPD in all carbon fixation types, however at higher temperatures only in C_4 and CAM plants but not in C_3 species. This is likely caused by the different stomatal conductance reactions to increased temperature. However, δ^2H_{ne} of sugar and cellulose was generally increased at higher temperature and VPD.

The results of δ^2H_{ne} of plant sugar are some of the first of its kind and together with other stable isotope (e.g. ^{18}O or ^{13}C) could lead to new insights into how certain plants behave in different climatic conditions. This could be useful for predicting the behaviour of ecosystems to climate change (e.g. rate of carbon fixation), or on smaller scales be used in agricultural research (e.g. find species that are more productive at higher temperatures and VPD).

The next steps could be to test a larger data set with more replicates and of different species, especially of C_4 plants. The application of the triple isotope measurement method could prove especially useful to achieve an overview over how hydrogen isotopes behave in relation to ^{18}O or ^{13}C, especially in NSC samples.

Chapter 7

Acknowledgements

I would like to express my gratitude to my supervisors Dr. Marco Lehmann and PhD Philipp Schuler and my faculty connection PD Dr. Guido Lars Bruno Wiesenberg, for their support and the opportunity to do this thesis with them. Furthermore, I would also like to thank Manuela Oettli for the reliable measurement of my samples and Loïc Schneider for his advice in the lab. And at last, my friends and family who encouraged and supported me over the years.

Chapter 8

References

Barbeta, A., Jones, S., Clavé, L., Wingate, L., Gimeno, T., Fréjaville, B., Wohl, S., & Ogée, J. (2018). Hydrogen isotope fractionation affects the identification and quantification of tree water sources in a riparian forest. *Hydrology and Earth System Sciences Discussions*, 1–29.

Black, C., & Osmond, C. (2003). Crassulacean acid metabolism photosynthesis: 'working the night shift'. *Photosynthesis research*, *76*, 329–341.

Boettger, T., Haupt, M., Knöller, K., Weise, S., Waterhouse, J., Rinne-Garmston, K., Loader, N., Sonninen, A., Jungner, H., Masson-Delmotte, V., Stievenard, M., Guillemin, M., Pierre, M., Pazdur, A., Leuenberger, M., Filot, M., Saurer, M., Reynolds, C., Helle, G., & Schleser, G. (2007). Wood cellulose preparation methods and mass spectrometric analyses of $\delta^{13}C$, $\delta^{18}O$, and nonexchangeable $\delta^{2}H$ values in cellulose, sugar, and starch: An interlaboratory comparison. *Analytical chemistry*, *79*, 4603–4612.

Buhay, W., Edwards, T., & Aravena, R. (1996). Evaluating kinetic fractionation factors used for reconstructions from oxygen and hydrogen isotope ratios in plant water and cellulose. *Geochimica Et Cosmochimica Acta - GEOCHIM COSMOCHIM ACTA*, *60*, 2209–2218.

Cernusak, L., Barbour, M., Arndt, S., Cheesman, A., English, N., Feild, T., Helliker, B., Holloway-Phillips, M., Holtum, J., Kahmen, A., McInerney, F., Munksgaard, N., Simonin, K., Song, X., Stuart-Williams, H., West, J., & Farquhar, G. (2015). Stable isotopes in leaf water of terrestrial plants. *Plant, Cell & environment*, *39*, 950–965.

Coplen, T. (2011). Guidelines and recommended terms of expression of stable-isotope-ratio and gas-ratio measurement results. *Rapid communications in mass spectrometry : RCM*, *25*, 2538–2560.

Cormier, M., Werner, R., Sauer, P., Gröcke, D., Leuenberger, M., Wieloch, T., Schleucher, J., & Kahmen, A. (2018). ^{2}H-fractionations during the biosynthesis of carbohydrates and lipids imprint a metabolic signal on the δ2h values of plant organic compounds. *New Phytologist*, *218*, 479–491.

DeNiro, M., & Epstein, S. (1981). Isotopic composition of cellulose from aquatic organisms. *Geochimica et Cosmochimica Acta*, *45*, 1885–1894.

Dulamsuren, C., & Hauck, M. (2021). Drought stress mitigation by nitrogen in boreal forests inferred from stable isotopes. *Global Change Biology*, *27*, 5211–5224.

Filot, M., Leuenberger, M., Pazdur, A., & Boettger, T. (2006). Rapid online equilibration method to determine the d/h ratio of non-exchangeable hydrogen in cellulose. *Rapid communications in mass spectrometry : RCM*, *20*, 3337–3344.

Fleta-Soriano, E., Pintó-Marijuan, M., & Munné-Bosch, S. (2015). Evidence of drought stress memory in the facultative cam, aptenia cordifolia: Possible role of phytohormones. *PloS one*, *10*, Article Nr.: e0135391.

Furze, M., Huggett, B., Aubrecht, D., Stolz, C., Carbone, M., & Richardson, A. (2018). Whole-tree nonstructural carbohydrate storage and seasonal dynamics in five temperate species. *New Phytologist*, *221*, 1466–1477.

Gatti, L., Basso, J., L.and Miller, Gloor, M., Domingues, L., Cassol, H., Tejada, G., Aragão, L., Nobre, C., Peters, W., Marani, L., Arai, E., Sanches, A., Corrêa, S., Anderson, L., Von Randow, C., S. C. Correia, C., Crispim, S., & Neves, R. (2021). Amazonia as a carbon source linked to deforestation and climate change. *Nature*, *595*, 388–393.

Gaudinski, J., Dawson, T., Quideau, S., Schuur, E., Roden, J., Trumbore, S., Sandquist, D., Oh, S., & Wasylishen, R. (2005). Comparative analysis of cellulose preparation techniques for use with ^{13}c, ^{14}c, and ^{18}o isotopic measurements. *Analytical chemistry*, *77*, 7212–7224.

Gehre, M., Geilmann, H., Richter, J. M., Werner, R., & Brand, W. A. (2004). Continuous flow $^2H/^1H$ and and $^{18}O/^{16}O$ analysis of water samples with dual inlet precision. *Rapid Communications in Mass Spectrometry*, *18*, 2650–2660.

Grossiord, C., Buckley, T., Cernusak, L., Novick, K., Poulter, B., Siegwolf, R., Sperry, J., & McDowell, N. (2020). Plant responses to rising vapour pressure deficit. *New Phytologist*, *226*, 1550–1566.

Hobson, K., & Wassenaar, L. (2018). *Tracking animal migration with stable isotopes - 2nd edition*.

Holden, N., Coplen, T., Bohlke, J., Tarbox, L., Benefield, J., Laeter, J., Mahaffy, P., O'Connor, G., Roth, E., Tepper, D., Walczyk, T., Wieser, M., & Yoneda, S. (2018). IUPAC periodic table of the elements and isotopes (IPTEI) for the education community (IUPAC technical report). *Pure and Applied Chemistry*, *90*, 1833–2092.

Inoue, T., Sunaga, M., Ito, M., Yuchen, Q., Matsushima, Y., Sakoda, K., & Yamori, W. (2021). Minimizing vpd fluctuations maintains higher stomatal conductance and photosynthesis, resulting in improvement of plant growth in lettuce. *Frontiers in Plant Science*, *12*, Article Nr.: 646144.

Johnson, M. (2016). Photosynthesis. *Essays In Biochemistry*, *60*, 255–273.

Kelly, S., Heaton, K., & Brereton, P. (2001). Deuterium/hydrogen isotope ratio measurement of water and organic samples by continuous-flow isotope ratio mass spectrometry using chromium as the reducing agent in an elemental analyser. *Rapid communications in mass spectrometry : RCM*, *15*, 1283–1386.

Kutschera, W., & Rom, W. (2000). Ötzi, the prehistoric iceman. *Nuclear Instruments and Methods in Physics Research Section B: Beam Interactions with Materials and Atoms*, *164-165*, 12–22.

Lauterbach, M., Billakurthi, K., Kadereit, G., Ludwig, M., Westhoff, P., & Gowik, U. (2016). C_3 cotyledons are followed by c_4 leaves: Intra-individual transcriptome analysis of salsola soda (chenopodiaceae). *Journal of Experimental Botany*, *68*, 161–176.

Leaney, F., Osmond, C., Allison, G., & Ziegler, H. (1985). Hydrogen-isotope composition of leaf water in C_3 and C_4 plants: Its relationship to the hydrogen-isotope composition of dry matter. *Planta*, *164*, 215–220.

Lehmann, M., Egli, M., Brinkmann, N., Werner, R., Saurer, M., & Kahmen, A. (2020). Improving the extraction and purification of leaf and phloem sugars for oxygen isotope analyses. *Rapid Communications in Mass Spectrometry*, *34*, Article Nr.: e8854.

Lehmann, M., Gamarra, B., Kahmen, A., Siegwolf, R., & Saurer, M. (2017). Oxygen isotope fractionations across individual leaf carbohydrates in grass and tree species. *Plant, Cell & Environment*, *40*, 1658–1670.

Lehmann, M., Vitali, V., Schuler, P., Leuenberger, M., & Saurer, M. (2020). More than climate: Hydrogen isotope ratios in tree rings as novel plant physiological indicator for stress conditions. *Dendrochronologia*, *65*, Article Nr.: 125788.

Leng, M., & Marshall, J. (2004). Palaeoclimate interpretation of stable isotope data from lake sediment archives. *Quaternary Science Reviews*, *23*, 811–831.

Li, S., Bashline, L., Lei, L., & Gu, Y. (2014). Cellulose synthesis and its regulation. *The Arabidopsis book / American Society of Plant Biologists*, *12*, Article Nr.: e0169.

Liu, J., Liu, W., An, Z., & Yang, H. (2016). Different hydrogen isotope fractionations during lipid formation in higher plants: Implications for paleohydrology reconstruction at a global scale. *Scientific Reports*, *6*, Article Nr.: 19711.

Luo, Y., Steinberg, L., Suda, S., Kumazawa, S., & Mitsui, A. (1991). Extremely low d/h ratios of photoproduced hydrogen by cyanobacteria. *Plant and Cell Physiology*, *32*, 897–900.

Luo, Y., & Sternberg, L. (1991). Deuterium heterogeneity in starch and cellulose nitrate of cam and c_3 plants. *Phytochemistry*, *30*, 1095–1098.

Merilo, E., Yarmolinsky, D., Jalakas, P., Parik, H., Tulva, I., Rasulov, B., Kilk, K., & Kollist, H. (2017). Stomatal vpd response: There is more to the story than aba. *Plant Physiology*, *176*, 851–864.

Naumann, G., Alfieri, L., Wyser, K., Mentaschi, L., Betts, R., Carrao, H., Spinoni, J., Vogt, J., & Feyen, L. (2018). Global changes in drought conditions under different levels of warming. *Geophysical Research Letters*, *45*, 3285–3296.

Richter, A., Wanek, W., Werner, R., Ghashghaie, J., Jäggi, M., Gessler, A., Brugnoli, E., Hettmann, E., Göttlicher, S., Salmon, Y., Bathellier, C., Kodama, N., Nogués, S., Søe, A., Volders, F., Sörgel, K., Blöchl, A., Siegwolf, R., Buchmann, N., & Gleixner, G. (2009). Preparation of starch and soluble sugars of plant material for the analysis of carbon isotope composition: A comparison of methods. *Rapid communications in mass spectrometry : RCM*, *23*, 2476–2488.

Roden, J., & Ehleringer, J. (2000). Hydrogen and oxygen isotope ratios of tree ring cellulose for field-grown riparian trees. *Oecologia*, *123*, 481–489.

Rodriguez-Celis, E., Jalbert, J., Duchesne, S., Arroyo, O., Rodriguez, L., Cross, J., & Lewand, L. (2017). On the experimental determination of the nitrogen content of thermally upgraded electrical papers. *IEEE Transactions on Dielectrics and Electrical Insulation*, *24*, 3092–3098.

Sanchez-Bragado, R., Serret, M., Marimon, R., Bort, J., & Araus, J. (2019). The hydrogen isotope composition δ^2H reflects plant performance. *Plant Physiology*, *180*, 793–812.

Saurer, M., Borella, S., & Leuenberger, M. (1997). $\delta^{18}O$ Of tree rings of beech (fagus silvatica) as a record of $\delta^{18}O$ of the growing season precipitation. *Tellus B*, *49*, 80–92.

Saurer, M., & Cherubini, P. (2021). Tree physiological responses after biotic and abiotic disturbances revealed by a dual isotope approach. *Tree physiology*, *42*, 1–4.

Schmidt, H., Werner, R., & Eisenreich, W. (2003). Systematics of ^{2}h patterns in natural compounds and its importance for the elucidation of biosynthetic pathways. *Phytochemistry Reviews - PHYTOCHEM REV*, *2*, 61–85.

Schuler, P., Cormier, R., M.and Werner, Buchmann, N., Gessler, A., Vitali, V., Saurer, M., & Lehmann, M. (2021). A high temperature water vapour equilibration method to determine non-exchangeable hydrogen isotope ratios of sugar, starch, and cellulose. *Plant, Cell & Environment*, 12–22.

Sharp, Z. (2007). *Principles of stable isotope geochemistry.*

Singhal, G., Renger, G., Sopory, S., Irrgang, K.-D., & Govindjee, G. (1999). *Concepts in photobiology: Photosynthesis and photomorphogenesis.*

Sternberg, L., DeNiro, M., & Johnson, H. (1984). Isotope ratios of cellulose from plants having different photosynthetic pathways. *Plant physiology*, *74*, 557–561.

Sternberg, L., DeNiro, M., & Johnson, H. (1986). Oxygen and hydrogen isotope ratios of water from photosynthetic tissues of cam and c_3 plants. *Plant physiology*, *82*, 428–431.

Tcherkez, G., Mahé, A., & Hodges, M. (2011). $^{12}C/^{13}C$ Fractionations in plant primary metabolism. *Trends in plant science*, *16*, 499–506.

Vreča, P., & Kern, Z. (2020). Use of water isotopes in hydrological processes. *Water*, *12*, Article Nr.: 2227.

Wang, L., Zhang, X., Ma, Y., Qing, Y., Wang, H., & Huang, X. (2019). The highly drought-tolerant pitaya (hylocereus undatus) is a non-facultative cam plant under both well-watered and drought conditions. *The Journal of Horticultural Science and Biotechnology*, *94*, 1–10.

Webster, G., Brown, W., & Smith, B. (1975). Systematics of photosynthetic carbon fixation pathways in euphorbia. *Taxon*, *24*, 27–33.

West, A., Patrickson, S., & Ehleringer, J. (2006). Water extraction times for plant and soil materials used in stable isotope analysis. *Rapid communications in mass spectrometry : RCM*, *20*, 1317–1321.

Winter, K. (2019). Ecophysiology of constitutive and facultative cam photosynthesis. *Journal of experimental botany*, *70*, 6495–6508.

Winter, K., Garcia, M., & Holtum, J. (2008). On the nature of facultative and constitutive cam: Environmental and developmental control of cam expression during early growth of clusia, kalanchoë, and opuntia. *Journal of experimental botany*, *59*, 1829–1840.

Xi, X. (2014). A review of water isotopes in atmospheric general circulation models: Recent advances and future prospects. *International Journal of Atmospheric Sciences*, 1385–1406.

Xia, Z., Zheng, Y., Stelling, J., J.and Loisel, Huang, Y., & Yu, Z. (2020). Environmental controls on the carbon and water (h and o) isotopes in peatland sphagnum mosses. *Geochimica et Cosmochimica Acta*, *277*, 265–284.

Yamori, W., Hikosaka, K., & Way, D. (2013). Temperature response of photosynthesis in c_3, c_4, and cam plants: Temperature acclimation and temperature adaptation. *Photosynthesis research*, *119*, 101–117.

Zarebanadkouki, M., Trtik, P., Hayat, F., Carminati, A., & Kaestner, A. (2019). Root water uptake and its pathways across the root: Quantification at the cellular scale. *Scientific Reports*, *9*, Article Nr.: 12979.

Chapter 9

Appendix

9.1 Raw data

Table 11: C_3 all averages and SDs

Species and Condition	**Water**			**Sugar**			**Cellulose**			**ϵbioHA**			**ϵbioHE**		
	Mean	SD	n	Mean	SD	n	Mean	SD	n	Mean	SD	n	Mean	SD	n
Abelmoschus esculentus 20° low	-43.2	1.2	3	-83.8	9.0	3	-29.5	5.3	3	-40.6	8.1	3	54.3	13.7	3
Abelmoschus esculentus 30° low	-12.5	1.0	3	-73.7	7.7	3	-35.0	10.5	3	-61.1	6.7	3	38.7	4.3	3
Abelmoschus esculentus 30° high	-18.0	2.0	3	-110.5	7.3	3	-63.4	10.6	3	-92.5	8.8	3	47.1	5.2	3
Anthurium sp. 20° low	-32.8	9.7	3	-70.7	2.1	3	-52.2	2.9	3	-38.6	7.2	2	18.4	3.1	3
Anthurium sp. 30° low	-35.0	2.5	2	-40.1	2.2	3	-39.6	12.2	3	-3.9	3.5	2	0.6	11.9	3
Anthurium sp. 30° high	-21.8	15.6	3	-25.9	4.3	3	-14.6	10.4	3	-4.1	12.7	3	11.3	14.0	3
Begonia maculata 20° low	-5.1	2.9	3	-145.1	14.1	3	-55.1	3.0	3	-140.1	14.5	3	90.0	12.6	3
Begonia maculata 30° low	-18.2	2.7	3	-106.8	8.9	3	-48.9	2.1	3	-88.6	11.6	3	58.0	10.4	3
Begonia maculata 30° high	3.4	3.4	3	-79.3	15.2	3	-21.6	8.8	3	-82.7	12.3	3	57.7	13.6	3
Begonia semperflorens 20° low	-26.6	4.4	3	-161.7	9.9	3	-42.3	6.3	3	-135.1	12.8	3	119.4	12.0	3
Begonia semperflorens 30° low	-29.6	1.3	3	-136.1	15.1	3	-54.1	5.5	3	-106.5	16.2	3	82.0	18.4	3
Begonia semperflorens 30° high	-18.7	6.3	3	-119.0	8.8	3	-40.2	13.3	3	-100.3	9.3	3	78.8	8.3	3
Cyperus sp. 20° low	-42.6	8.3	3	-86.6	10.2	3	-39.6	3.4	3	-44.1	17.4	3	47.0	10.4	3
Cyperus sp. 30° low	-59.1	2.1	3	-114.6	14.2	3	-76.4	1.3	3	-55.5	15.9	3	38.2	14.1	3
Cyperus sp. 30° high	-6.7	3.4	3	-65.9	3.8	3	-27.4	3.3	2	-59.3	4.1	3	36.4	3.8	2
Hordeum vulgare 20° low	-28.8	4.8	3	-187.4	3.5	2	-94.2	7.0	3	-161.2	1.4	2	89.7	1.4	2
Hordeum vulgare 30° low	-33.1	0.7	3	-112.0	13.0	3	-41.1	2.4	3	-78.9	13.0	3	70.9	12.6	3
Hordeum vulgare 30° high	-30.3	1.9	3	-74.8	5.1	3	-59.0	4.9	3	-44.6	6.9	3	15.8	8.5	3
Oryza sativa 20° low	-43.2	0.9	3	-76.6	8.6	3	-37.4	3.2	3	-33.4	7.7	3	39.2	8.8	3
Oryza sativa 30° low	-48.8	2.1	3	-102.8	2.5	3	-54.3	4.3	3	-54.0	3.9	3	48.5	2.8	3
Oryza sativa 30° high	-42.9	3.2	3	-116.9	3.1	3	-47.7	3.3	3	-74.0	5.4	3	69.1	0.5	3
Quercus pupescens 20° low	-30.0	2.8	3	-69.3	1.7	3	-48.4	4.2	3	-39.3	3.0	3	20.9	2.6	3
Quercus pupescens 30° low	-42.1	4.0	3	-118.4	7.5	3	-85.8	3.1	3	-76.2	5.9	3	32.6	4.5	3
Quercus pupescens 30° high	-20.3	1.9	3	-86.9	10.9	3	-43.1	9.0	3	-66.6	12.7	3	43.8	3.9	3
Salvia hispanica 20° low	-47.8	1.1	3	-126.4	27.9	2	-61.6	17.7	3	-77.9	27.3	2	55.2	19.2	2
Salvia hispanica 30° low	-27.2	3.0	3	-64.1	7.1	2	-36.3	4.3	3	-37.6	10.9	2	26.4	2.1	2
Salvia hispanica 30° high	-29.3	0.5	3	-91.8	4.6	3	-49.8	3.9	3	-62.5	4.2	3	42.0	1.3	3
Zantedeschia athiopica 20° low	-25.1	1.9	3	-74.1	8.0	3	-53.3	6.9	3	-49.0	7.9	3	20.8	4.8	3
Zantedeschia athiopica 30° low	-48.8	2.2	3	-90.4	13.7	3	-51.7	4.9	3	-41.6	15.5	3	38.7	10.3	3
Zantedeschia athiopica 30° high	-22.7	7.3	3	-14.1	8.2	3	-28.4	1.8	3	8.6	3.8	3	-14.4	7.2	3
MEAN:	-29.5	14.8	89	-93.1	36.7	87	-48.0	18.1	89	-64.8	38.2	85	45.6	29.6	86

Table 12: C_4 all averages and SDs

Species and Condition	**Water**			**Sugar**			**Cellulose**			**ϵbioHA**			**ϵbioHE**		
	Mean	SD	n	Mean	SD	n	Mean	SD	n	Mean	SD	n	Mean	SD	n
Amaranthus tricolor 20° low	-18.1	2.3	3	-38.1	5.5	3	17.4	5.6	3	-19.9	6.9	3	55.4	10.2	3
Amaranthus tricolor 30° low	-25.2	2.5	3	-39.2	5.2	3	1.3	12.9	3	-14.0	7.7	3	40.5	17.7	3
Amaranthus tricolor 30° high	-6.0	3.2	3	-31.5	4.2	3	23.3	8.5	3	-25.5	1.1	3	54.8	11.0	3
Pennisetum glaucum 20° low	-50.6	4.0	3	-17.5	9.6	3	11.5	9.6	3	33.1	11.8	3	29.0	4.8	3
Pennisetum glaucum 30° low	-40.0	1.9	3	-17.6	2.6	3	6.2	5.6	3	22.4	4.1	3	23.8	3.3	3
Pennisetum glaucum 30° high	-38.8	2.3	3	-18.9	9.1	3	18.9	10.5	3	19.9	7.7	3	37.9	2.2	3
Setaria italica 20° low	-46.3	1.5	3				7.1	12.1	3						
Setaria italica 30° low	-29.6	2.2	3				10.8	4.6	3						
Setaria italica 30° high	-26.3	4.6	3	-36.3	0.7	3	4.1	16.9	3	-10.0	3.9	3	40.4	16.2	3
Sorghum bicolor 20° low	-55.5	4.6	3	-36.3	15.8	3	-4.9	17.2	3	19.2	14.4	3	31.3	7.2	3
Sorghum bicolor 30° low	-40.9	7.7	3	-16.9	12.5	3	-0.4	7.2	3	24.0	5.3	3	16.5	5.3	3
Sorghum bicolor 30° high	-32.4	4.6	3	-33.8	9.0	3	10.5	1.3	2	-1.4	13.6	3	47.0	12.0	2
Zea mays 20° low	-48.1	2.6	3	-42.2		1	-5.4	13.4	3	3.2		1	25.3		1
Zea mays 30° low	-42.1	2.3	2	-32.2	13.3	3	-9.0	12.4	2	2.3	0.9	3	33.6	8.1	3
Zea mays 30° high	-38.9	3.6	2	-36.0	17.2	3	-7.7	9.3	3	8.9	15.9	3	28.3	10.9	3
MEAN:	-33.3	13.8	52	-32.0	12.6	43	6.9	13.1	48	-0.2	22.5	43	39.2	16.4	41

Table 13: CAM all averages and SDs

Species and Condition	**Water**			**Sugar**			**Cellulose**			**ϵbioHA**			**ϵbioHE**		
	Mean	SD	n	Mean	SD	n	Mean	SD	n	Mean	SD	n	Mean	SD	n
Amaranthus caudatus 20° low	-13.9	3.6	3	-49.0	7.1	3	18.2	4.4	3	-35.2	7.4	3	67.3	6.3	3
Amaranthus caudatus 30° low	-18.1	1.3	3	-41.7	2.8	3	13.5	15.7	2	-23.6	4.0	3	56.2	18.9	2
Amaranthus caudatus 30° high	-33.0	5.1	3												
Aptenia cordifolia 20° low	-13.4	4.0	3	-97.2	3.8	3	-51.4	0.2	2	-83.7	1.4	3	57.4	21.6	3
Aptenia cordifolia 30° low	-17.7	1.0	2	-68.9	13.0	3	-45.1	11.1	3	-50.8	19.5	2	23.8	4.7	3
Aptenia cordifolia 30° high	0.5	1.2	3	-75.6	5.6	3	-31.0	8.0	2	-76.1	4.4	3	55.9	17.1	3
Delosperma cooperi 20° low	-19.3	0.5	3	-91.6	8.4	3	-13.8	9.3	3	-72.4	8.8	3	77.8	5.0	3
Delosperma cooperi 30° low	-23.7	1.3	3	-82.2	6.7	3	4.2	15.4	2	-58.5	6.2	3	71.9	25.9	3
Delosperma cooperi 30° high	-21.0	2.0	3	-104.7	7.7	3	-25.0	2.7	3	-83.8	6.3	3	79.7	8.3	3
Euphorbia pulcherrima 20° low	-21.7	1.4	3	-21.8	9.7	3	-2.1	18.6	3	-0.1	8.3	3	19.7	21.0	3
Euphorbia pulcherrima 30° low	-29.8	3.7	3	-40.6	18.1	3	-17.6	8.3	3	-10.8	21.7	3	23.1	21.5	3
Euphorbia pulcherrima 30° high	-33.7	4.6	3	-32.6	15.3	3	1.2	8.1	3	1.1	15.8	3	33.8	8.1	3
Hylocereus sp. 20° low	-11.5	8.1	3	34.4	10.1	3	58.7	8.4	3	46.0	12.2	3	24.2	1.8	3
Hylocereus sp. 30° low	-5.5	6.3	3	68.5	4.3	3	65.1	14.9	3	74.0	7.7	3	-3.3	10.5	3
Hylocereus sp. 30° high	14.0	5.9	2	96.4	5.9	3	83.8	10.2	3	85.1	0.9	2	-12.6	4.4	3
Phalaenopsis 20° low	-8.3	1.2	3	40.9	10.0	3	40.7	10.0	3	49.2	9.7	3	-0.1	8.8	3
Phalaenopsis 30° low	-18.5	8.6	3	25.4	16.8	3	36.0	13.2	3	43.9	9.0	3	10.6	30.0	3
Phalaenopsis 30° high	-2.0	1.1	3	56.5	3.5	3	37.4	14.8	2	58.5	4.2	3	-1.8	33.2	3
Rhipsalis sp. 20° low	-8.9	2.8	3	46.0	5.1	3	37.3	8.5	3	54.9	7.6	3	-8.7	9.0	3
Rhipsalis sp. 30° low	-8.6	4.2	3	23.4	11.8	3	-7.4	4.4	3	32.1	7.7	3	-30.8	10.4	3
Rhipsalis sp. 30° high	27.6	2.3	3	57.2	7.6	3	21.2	12.0	3	29.6	7.0	3	-35.9	19.2	3
Salsola soda 20° low	-14.6	1.8	3	12.2	2.8	3	39.3	19.4	3	26.8	4.3	3	27.2	21.6	3
Salsola soda 30° low	-31.3	1.6	3	-10.2	2.3	3	51.1	6.8	3	21.1	3.5	3	61.3	6.9	3
Salsola soda 30° high	-13.7	1.2	3	17.0	12.6	3	99.8	9.6	3	30.6	12.7	3	82.8	21.6	3
Sedum sp. 20° low	-3.0	12.7	3	-0.4	1.5	3	23.2	10.9	3	2.5	11.5	3	23.7	9.9	3
Sedum sp. 30° low	-16.0	2.0	3	16.5	2.6	3	56.9	8.3	3	32.5	1.1	3	40.4	6.3	3
Sedum sp. 30° high	29.1	1.9	3	45.3	8.3	3	97.5	11.5	3	16.2	10.2	3	52.2	19.6	3
Senecio sempervivus 20° low	2.4	3.4	3	-36.6	11.2	2	10.6	15.3	3	-40.3	14.8	2	34.8	13.0	3
Senecio sempervivus 30° low	-19.0	3.1	3	-19.6	5.5	3	64.2	15.7	3	-0.7	8.6	3	83.8	13.7	3
Senecio sempervivus 30° high	-4.6	1.5	3	-12.0	5.7	3	86.1	16.2	3	-7.4	7.1	3	98.1	10.5	3
MEAN:	-10.3	15.6	79	-5.3	55.4	80	28.6	42.8	77	4.7	48.8	78	32.9	38.5	81

Chapter 10

Declaration of Independence

Personal declaration: I hereby declare that the submitted Thesis is the result of my own, independent work. All external sources are explicitly acknowledged in the Thesis.

Zurich, April 30, 2022
Oliver Rehmann